AD NUMBER

AD911778

NEW LIMITATION CHANGE

TO

Approved for public release, distribution unlimited

FROM

Distribution authorized to U.S. Gov't. agencies only; test and evaluation; Feb 1973. Other requests shall be referred to Air Force Armament Laboratory [DLRV], Eglin Air Force, Florida 32542.

AUTHORITY

AFAL Itr, 24 Oct 1975

AD911778

AFATL-TR-73-26

STUDY OF THE TERMINAL EFFECTS OF PYROPHORIC METAL FRAGMENTS

ORDNANCE RESEARCH, INC.

TECHNICAL REPORT AFATL-TR-73-26
FEBRUARY 1973

AIR FORCE ARMAMENT LABORATORY
AIR FORCE SYSTEMS COMMAND • UNITED STATES AIR FORCE
EGLIN AIR FORCE BASE, FLORIDA

Study Of The Terminal Effects Of Pyrophoric Metal Fragments

Hal R. Waite
Theodore B. Gortemoller

FOREWORD

This report was prepared by Ordnance Research, Inc., Fort Walton Beach, Florida 32548, under Contract Number F08635-71-C-0020 with the Air Force Armament Laboratory, Eglin Air Force Base, Florida. Mr. Francis N. McMillan (DLRV) was program manager for the Armament Laboratory. Mr. Theodore B. Gortemoller was program manager for the contractor. This study began in September 1970 and was completed in February 1973.

This technical report has been reviewed and is approved.

CHARLES K. ARPKE, Lt Colonel, USAF
Chief, Weapons Effects Division

ABSTRACT

Thirty-three metals and alloys having pyrophoric properties were surveyed for applicability as gun-launched kinetic energy penetrators, incendiaries, and fuel igniters. Using actual samples physical properties were determined, ignition-combustion temperature/burn time profiles were established, and dynamic terminal effects were tested. Six pyrophoric metals were tested against simulated characteristic targets. The results of all testing are tabulated, and recommendations are made for an advanced development program.

(The reverse of this page is blank)

TABLE OF CONTENTS

LIST OF TABLES

LIST OF TABLES (CONCLUDED)

LIST OF FIGURES

LIST OF FIGURES (CONCLUDED)

(The reverse of this page is blank)

SECTION I

INTRODUCTION AND SUMMARY

Pyrophoric materials have many applications as kinetic energy penetrators and supplemental penetrators for weapons systems. They offer the advantages of design simplicity, good penetration, and inherent incendiary effects. However, the major portion of work in this field has been done with a cut-and-try approach using a limited number of favored materials rather than through an orderly program of complete analysis and test of the entire range of pyrophoric metals. The objective of this program is to develop quantitative data descriptive of the terminal effects of gun-launched state-of-the-art reactive metal penetrators.

Prototype munitions employing pyrophoric fragments as penetrators are now being produced. Some of these weapons were submitted for empirical testing against simulated generic targets. These tests are useful, but because the competing munitions employ different materials in different configurations, little will be learned about the basic effects. A comparison of several of the most promising materials in carefully controlled tests using various standard configurations is urgently needed. Heat energy and duration determinations of pyrophoric penetrators are almost non-existent.

The approach in this program was to survey a wide range of alloys, fabricate samples, determine physical properties, establish static time/temperature combustion profiles, and test dynamic terminal effects of each. From these tests, six reactive metal compositions were selected for further testing against simulated fuel-containing targets.

Fragment impact velocities were varied from 1000 to 5000 feet per second in 500 feet per second increments.

Target materials were aluminum, carbon steel, and titanium. The target thicknesses selected were representative of components common to targets, especially aircraft. In addition, tests were conducted to compare the fire-starting capability of the six materials selected for final evaluation.

The terminal effects data will be valuable in determining the vulnerability of foreign targets to this fragment/incendiary-type penetrator. These lethality determinations will establish the potential for further development of munitions employing pyrophoric penetrators or fragments.

As a base constituent for alloying, cost-effective commercially available mixed rare earths (MRE) alloy (also known as mischmetal) was used. In general, MRE consists of about 50 percent cerium with the balance being a mixture of other rare earths of the cerium group of lanthanides. The exact percentages depend on the source ore and on refining and recovery processes. The composition of mixed rare earths from bastnasite ore sources falls within the following proportions:

Cerium	48 - 52 %
Lanthanum	23 - 27 %
Neodymium	15 - 17 %
Praseodymium	5 - 7 %
Other Rare Earths	1 - 3 %

Physical properties testing disclosed that the alloys of MRE containing 4% or more of added metal are brittle. Subsequent terminal effects testing of gun-launched penetrators against steel and titanium target plates proved these alloys would brittle-fracture and at higher impact velocities exhibit the same failure mode against an aluminum target. Generally, peak temperature and heat output at low velocities are superior when compared with metals such as depleted uranium, thorium, titanium, zirconium, or zirconium-tin, which do not suffer fracture or spall at impact velocities below 3500 feet per second.

Thermal properties testing (static) yielded a wide range of auto-ignition temperatures, peak temperatures, and burn times. Comparing and matching these results with the physical test results gives a good basis for decision on which alloys are useful for gun systems and which are more suitable for explosive dissemination.

Qualitative data on oxidation and corrosion rates were also obtained.

The results of this program have demonstrated that the mixed rare earth alloys will more consistently initiate self-sustaining fires and perform well at significantly lower impact velocities than the other pyrophoric metals tested, as can be seen in Figures 1 through 3. These figures depict the total thermal energy versus projectile velocity for each of the three target plate materials and thicknesses. It has also been shown that a careful selection should be made to tailor the alloy to the delivery system in order to assure maximum weapon effectiveness.

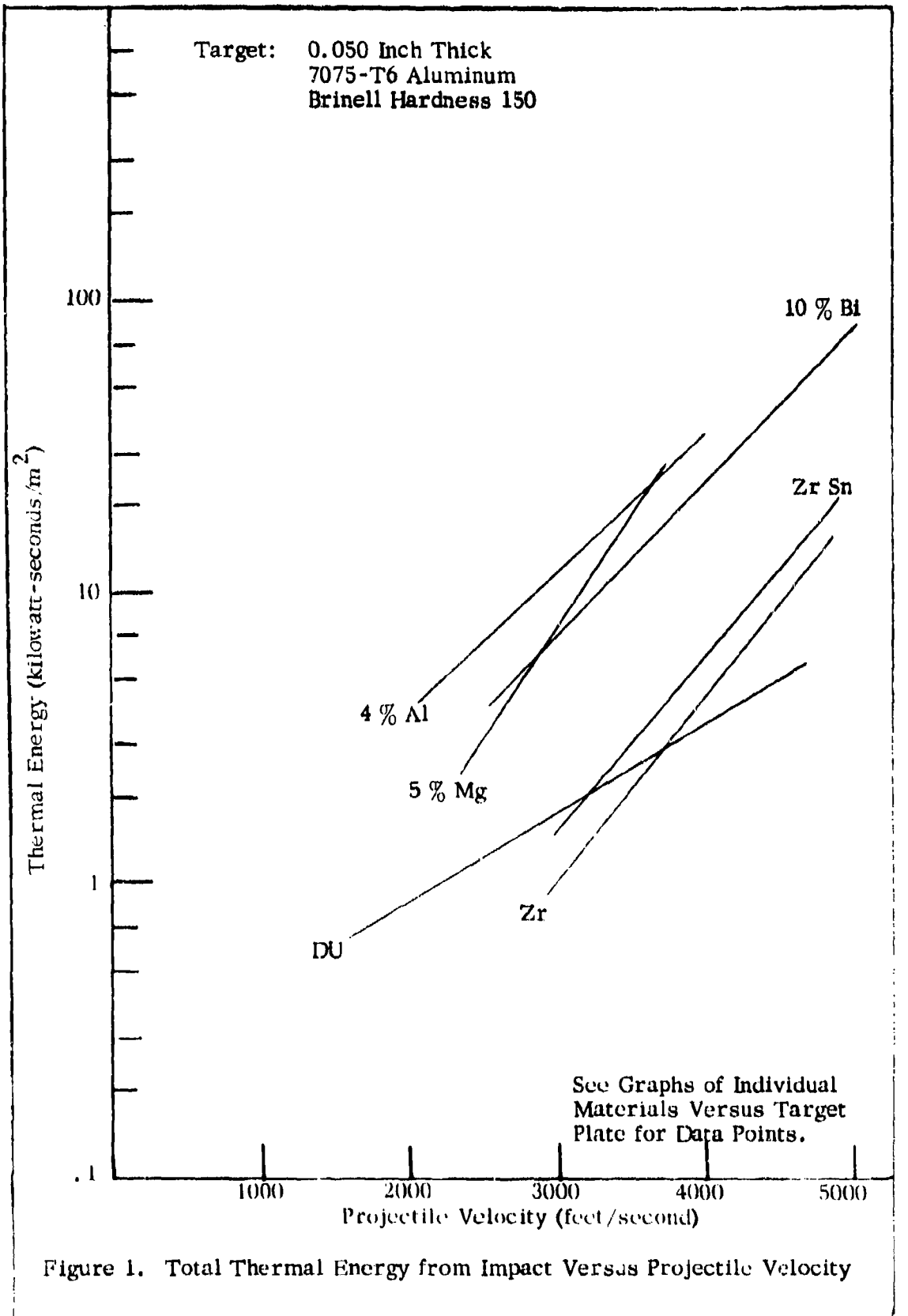

Figure 1. Total Thermal Energy from Impact Versus Projectile Velocity

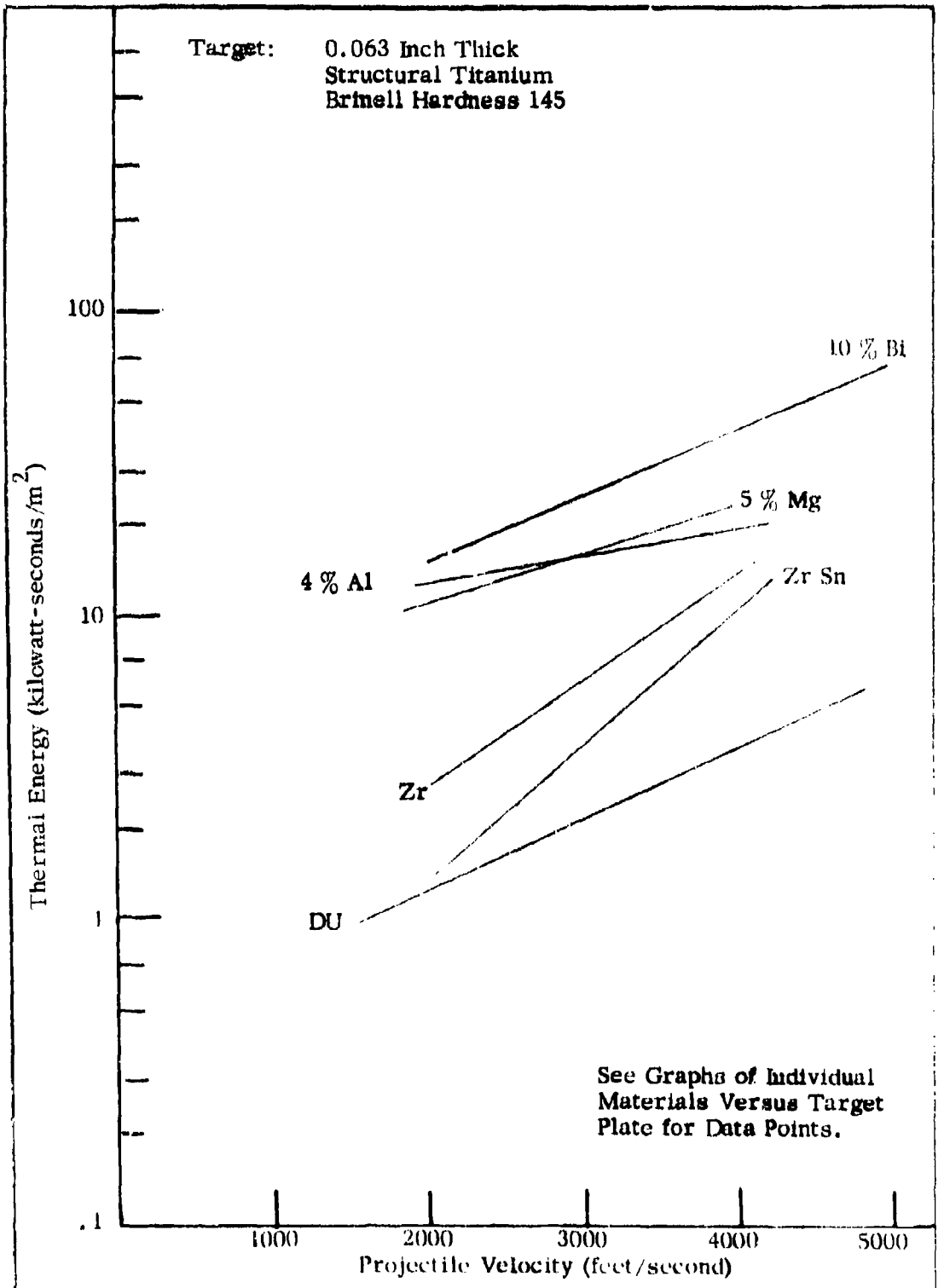

Figure 2. Total Thermal Energy from Impact Versus Projectile Velocity

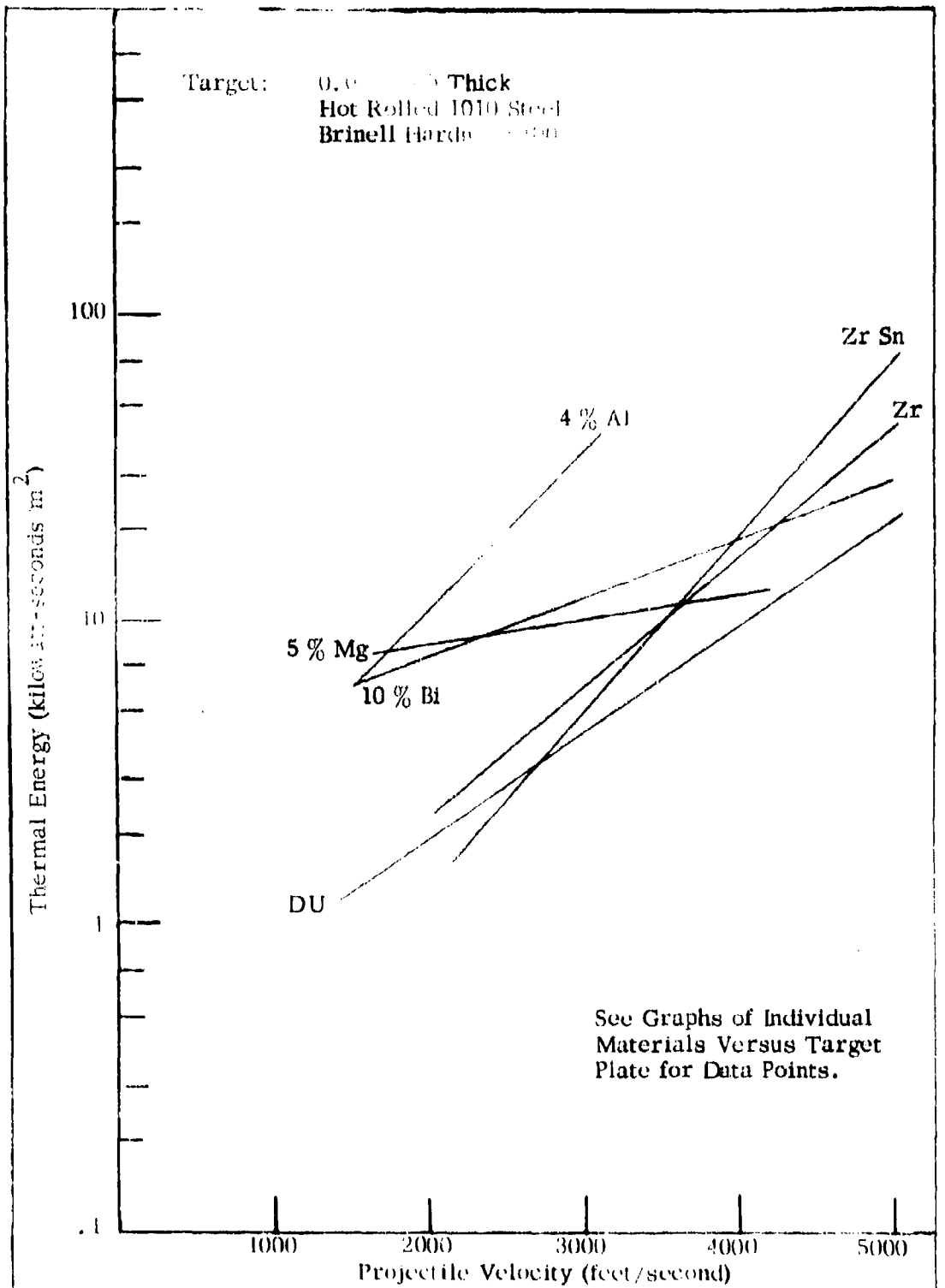

Figure 3. Total Thermal Energy from Impact Versus Projectile Velocity

SECTION II

TECHNICAL DISCUSSION

Mechanism of Ignition

The secondary incendiary effects of massive pyrophoric metal penetrators offer certain advantages in the defeat of aircraft or vehicle targets and the venting and ignition of drummed POL. Previous developments have been based on the use of pyrophoric metal powders as fuels for exothermic pyrotechnic compositions (powdered fuel with oxidizers) for primary incendiary effect or the use of explosively launched fragments either of pyrophoric metal per se, or steel fragments augmented by pyrophoric metal as case liners or explosive additives.

The critical period of ignition of diesel fuel and, to a lesser extent, gasoline is the 10-to 100-millisecond period following fragment impact. Hydrostatic shock of the fuel body exposes a rapidly expanding vapor or fuel droplet cloud. The fuel-air mixture within the flammable limits forms and dissipates within a period of 10- to 200-milliseconds. Subsequent to this time interval, only pooled fuel is available for ignition requiring a high-temperature extended-burning ignition source, especially for low volatile fuels. Most reliable ignition of fuel by this mechanism will therefore occur when the fragmentation and incendiary capabilities are incorporated in a single munition.

The damage or fire-starting potential of an alloy or pure metal as a pyrophoric kinetic energy penetrator depends upon mechanically induced pyrophoricity. Friction is the mechanism employed and is induced by impact and abrasion with the target metal plate while penetrating and the internal frictional shear forces between metallic phases during penetrator failure. With the exception of the reported solid solution of thorium in MRE, these rare earth elements form stable intermetallic compounds which are insoluble in the MRE solidus. Thus, two phases are formed. Frictional forces and heating on shear due to impact cause internal pyrophoricity, brittle fracture, and ignition of the spalled metal. Elements or solid solutions do not exhibit this second mode of induced pyrophoricity. Impact and abrasion are dependent on reaction with the target and are therefore dependant on target material. Targets of steel and, to a lesser extent, titanium provide significant impact resistance and abrasion when penetrated and are therefore excellent targets for this type of penetrator. Aluminum with low ultimate yield strength does not provide sufficient impact resistance or abrasion on penetration and therefore does not supply sufficient heat to initiate the reaction at lower velocities.

Intergranular friction or internally induced pyrophoricity during brittle fracture of a penetrator is not completely target-dependent and adds significantly to the initial event with the added bonus of supplying many burning particles as a residual effect covering several milliseconds. The persistence of this residual effect is dependent on two conditions: (1) the size of the residual particles, and (2) the burning rate of the particular alloy. Both of these conditions are pyrophoric metal or alloy-dependent. All of the MRE alloys and the MRE in the as-cast condition are subject to brittle failure; a number were shown to break into sufficient large particle sizes to be significant. Of these,

there are several that were determined to have sufficiently long burning times to be of interest. All react at a temperature of at least 2300°C, which is sufficient for the incendiary purpose of fuel ignition. Zirconium, depleted uranium, and titanium are subject to ductile failure and are therefore almost completely dependent on target/penetrator interaction with accompanying limited burning persistence.

Target Effects

In selecting a representative target, it is important to understand the mechanisms for initiation of fuel fires and/or explosions due to impact by incendiary kinetic energy penetrators. Penetration of a projectile into the liquid space of a fuel tank provides energy for the formation of a fuel-air cloud which can be ignited by the dispersed incendiary particles if certain criteria (which are discussed below) exist. If not directly ignited by the initial penetrator, the leaking fuel can subsequently be ignited by other projectile impacts nearby. Projectile impacts into the ullage volume of fuel tanks provide another means of initiation of a self-sustaining fire of lesser intensity.

Early experiments concerning fuel ignition by incendiary penetration monitored by Fastax camera coverage resulted in the postulation that the following conditions are essential to successful ignition of a fuel target. [1]

1. Penetration of the fuel cell by a projectile.
2. Emergence of the fuel from the fuel cell.
3. Mixture (however incomplete) of fuel and air in combustible proportions.
4. Existence of an adequate igniter in the zone of combustibility.
5. Propagation of the flame throughout the target.

The mechanism of hydrocarbon ignition and combustion has been analyzed extensively over the past few years. During the latter part of World War II, British scientists studied the processes involved in the release of fuel from aircraft fuel tanks and in the diffusion and ignition of these fuels. In general, it was found that the relative volatility of a fuel is the most important single factor in determination of the ignition and flame propagation qualities of a fuel spray. The probability of the incidence of propagated flame in fuel-air mixtures at temperatures below the flash-point is nil unless the fuel is dispersed in a manner which favors aerosol formation.

It has been confirmed experimentally that a condition of flammability exists in a fuel-air system in equilibrium when the temperature, which controls the concentration of the fuel-vapor and air mixture, lies between certain limits known as the upper and lower limits of flammability. With a typical gasoline, this zone of flammability occurs at fuel temperatures of approximately -35 to -40°F at sea level. With kerosene, the flammability zone for the equilibrium

---

1. G. H. Custard, G. Francis, and W. Schmackenberg, Small Arms Incendiary Ammunition, A Review of the History and Development, AD 159323, II, p. 152.

mixture occurs with fuel temperatures between 100°F to 110°F at sea level. Within the above flammability zones, a fire or explosion can result from contact with an ignition source. The flash point of a given fuel is defined as the lower limit of the flammability zone. These considerations apply in this case to the flammability temperature limits in closed system such as the ullage volume in closed fuel cells or tanks.

The lower and upper concentration limits of flammability indicate the percentage of combustible gas in air, below which and above which flame will not propagate. When flame is initiated in mixtures having compositions within these limits, it will propagate and therefore the mixtures are flammable.

It is generally postulated that combustion of hydrocarbons (1) occurs in the vapor phase, (2) is a chain reaction dependent upon the formation of unstable species such as free radicals, and (3) can occur only within certain well-defined limits of concentration. To ignite a system of air and liquid hydrocarbon fuel, therefore, enough energy must be provided to establish the above conditions at some point in the system. Flame will not be propagated, however, if the energy released following ignition is not great enough to spread the required ignition conditions to adjacent areas, or if too much energy is lost to the surroundings.

Theoretical consideration of the incendiary burst has been approached from several standpoints. Fundamentally, of course, the burst produced by the incendiary is nothing more than a source of ignition for fuel fires. In itself it is incapable of directly destroying a target because it is unlikely that an incendiary burst of sufficient intensity or duration to weaken or kindle aircraft structures can be produced by small incendiary kinetic energy penetrators. With reference to the incendiary burst as a source of ignition for fuel-air mixtures, the intensity, spatial distribution and duration of the burst determine the probability of the desired ignition assuming that an ignitable mixture is within the immediate impact area.

The position of the burst is determined primarily by the [illegible]sivity of the alloy and its ability to carry through target areas of effecti[illegible]ath. This phenomenon has been found important to the effectiveness of spark-producing incendiary compositions, because, as they spread throughout a target area, many individual ignition sources tend to produce a very large volume of effective burst.

A variety of attempts has been made to determine the minimum ignition temperatures for different fuels. A standard experimental procedure for such determinations involves confinement of the fuel-vapor and air mixture in a suitable container and heating and application of external ignition source at timed intervals until the mixture ignites. There exists, however, an ignition lag which is dependent upon several variables; thus, the measured flash point is not indicative of the temperature and thermal flux required for sustained combustion.

The test target configurations used during final evaluation were selected to be representative of a typical target as it would appear to the munition when delivered from an aircraft in a tactical environment.

With single projectiles, the geometry of the target setup is important in providing a means to confine both the incendiary particles and the fuel-air cloud

in the target area to increase the probability of achieving conditions suitable for combustion as in the real case configuration. With multiple hits in the area, target geometry is not as critical a factor but should not be overlooked. The target geometries for analysis in the final phase of the present program have been carefully selected to simulate the actual target configuration and structural confinement.

Characteristics of Pyrophorics

For practical munitions manufacture and storage considerations, the workability and oxidation resistance of the pyrophoric materials must be of increasing importance. Being brittle in nature, the mixed rare earths in the as-cast condition do not lend themselves to cold working. Extrusion at below the melting point, followed by an optional annealing cycle, increases elongation to between 25 and 40 percent and allows further cold working. Mixed rare earth alloys of 4 percent or greater added metal may be extruded; however, elongation is not increased. Titanium, zirconium, and Zircaloy (sometimes referred to as zirconium-tin) with a maximum tin content of 2.5 percent do not display this brittleness and have good cold and hot fabricability. Machinability of the MRE alloys is generally excellent, thus forming these materials by inert atmosphere casting with subsequent machining to finished dimensions is easily practical.

Oxidation and hydration of cerium and the mixed rare earths is fairly rapid and the product is in the form of a loose powdery scale. Many alloying materials eliminate this tendency as shown in Table I. This storage stability of zirconium and Zircaloy is excellent.

Selection of Materials

Textbook references on rare earths and their alloys are limited in availability. The most comprehensive texts are published under the auspices of the Atomic Energy Commission edited by members of the facility of the Ames Laboratory, Iowa State University.[2,3]

These texts are excellent sources for binary alloy phase diagrams; however, little information is given on the metallurgical properties. Limited assumptions may be made on the basis of general alloying theory and a knowledge of the effects of differences in atomic radii and electronegativities in solid solution formation. These latter effects can be graphically analyzed by means of a Darken and Gurry plot of the element electronegativity and atomic radius. Proximity of elements to the rare earth group would be favorable for solid solution formation and superior low temperature workability. This latter characteristic is not necessary in the fabrication of the penetrators for the present study; however, these alloys should demonstrate increased impact

---

2. The Rare Earths, ed. by F. H. Spedding and A. H. Daane, John Wiley and Sons, New York (1961)

3. Rare Earth Alloys, Karl A. Gschneidner, Jr., D. Van Nostrand Co., Princeton, N. J. (1961)

TABLE I. COMPARATIVE OXIDATION RESISTANCE OF PYROPHORIC METALS

Uncontrolled Storage Stability	Alloy No.	Composition
No appreciable surface discoloration	12	98% MRE +2% Vanadium
	19	95% MRE + 5% Magnesium
	22	Zirconium
	27	Titanium
	31	79% MRE + 3% Aluminum +3% Magnesium + 15% Lead
Minor surface discoloration	14	90% MRE + 10% Bismuth
	23	68% MRE + 32% Zinc
	28	96% MRE + 4% Iron
	29	96% MRE + 4% Aluminum
	30	92% MRE + 8% Manganese
	32	91% MRE + 9% Magnesium
Major surface discoloration	4	90% MRE + 10% Copper
	7	Thorium
	8	Uranium
	13	87% MRE + 13% Zinc
	16	50% MRE + 50% Lead
	Methenalloy	Proprietary
Minor surface scale	3	94% MRE + 6% Nickel
	5	93% MRE + 7% Cobalt
	15	94% MRE + 2% Cobalt + 2% Nickel + 2% Iron
	26	95.5% MRE + 4.5% Zinc
Major surface scale	1	Mixed Rare Earths
	2	Cerium 90 - 95% enriched MRE
	6	85% MRE + 15% Thorium
	9	94% MRE + 6% Calcium
	10	96% MRE + 4% Indium
Major surface powdering (oxidation)	11	94% MRE + 3% Cobalt + 3% Iron
	17	95% MRE + 5% Manganese
	18	97% MRE + 3% Tin
	20	98% MRE + 2% Lead
	24	85% MRE + 15% Lead
	25	98% MRE + 2% Cobalt

toughness and resistance to spall. This consideration was initially considered critical for penetration and residual mass; however, the kinetics of penetration or the extreme stress rate on penetration does not produce the expected or theoretical brittle fracture failure mode at the target surface. This result is apparent in the data given in the sequel. Of the readily available elements, it would be expected that only calcium, indium, magnesium, hafnium, cadmium, sodium, and thorium will show significant solubility. The phase diagrams of the systems, however, show less than the expected solid solubility.

Another parameter affecting low-temperature workability and resistance to impact is the crystal structure of the elemental metal. Lanthanum, praseodymium, and neodymium have the hexagonal, lanthanum type of structure. The room temperature structure for cerium is the face-centered cubic, copper type. The cold workability (or as first presumed, the penetration capability) of the latter type of structure is greater because of the increased degrees of freedom in slippage between crystal planes. The cubic structure does not show anisotropic behavior. Cerium-enriched mixed rare earths (90 to 95%) were therefore evaluated.

The selection of the MRE alloys was made on the basis of an analysis of the phase diagrams published in the referenced literature. Several criteria were chosen for the selection of alloys, all based on a combined analysis of the phase diagrams of both cerium and lanthanum inasmuch as the phase diagrams of elements and mixed rare earths are not available. Alloying elements such as tantalum and other refractory metals that markedly increased the liquidus or melt temperature at low percentage concentrations were not considered; cost of high temperature casting and loss of volatile rare earths are complications. Expensive alloying elements or source materials, with the exception of thorium, were eliminated from consideration. Many alloys were chosen to correspond to a eutectic composition; these melting point minima give a constant temperature phase transition between liquidus and solidus. The casting is thus more homogeneous than for compositions that exhibit a wide liquidus-solidus temperature range. The rare earth alloy phase diagrams were also surveyed for the characteristic of decreasing solubility of the solid intermetallic phase in the solidus with decreasing temperature. Heat-treatable ferrous alloys show this characteristic and it was postulated that heat treatment of certain rare earth alloys was possible; however, no hardness increase for any alloy was effected by these attempts.

SECTION III

PHYSICAL AND THERMOCHEMICAL

There were six distinct test item configurations for the program. The first three for the determination of physical properties were the standard ASTM tensile test specimen (as shown in Figure 4), the Charpy impact unnotched test specimen (Figure 5), and a Rockwell hardness test specimen. These tests furnished the basic physical properties of all pyrophoric alloys and elements considered which are tabulated in Table II.

The static time-temperature profiles (Table III and Figure 6) were obtained using an optical pyrometer and a small electric furnace (Figure 7). The test specimens used were 0.25 inch by 0.25 inch right circular cylinders of the configuration specified for the dynamic tests. They were placed in a small crucible in the furnace, a quartz glass face was installed in place of the furnace door and power applied to the furnace at a predetermined rate. The temperature of the specimen was monitored by the optical pyrometer as it was heated to the autoignition temperature (indicated by an increasing slope in the temperature-time trace). At this time, the furnace was turned off and the burn temperature and burn time of the specimen monitored. For this experiment, burn time was defined as time from autoignition until the specimen cooled to 400°C. In some cases, autoignition could not be achieved in the oven at a maximum temperature of 800°C, and other means were adopted in an effort to obtain higher temperature autoignition data. This procedure was to leave the round in the oven with the pyrometer in place as previously described; the round was then heated with an external propane burner source and the maximum temperature achieved was read on the pyrometer and recorded.

The terminal effects of the pyrophoric penetrators were measured by a test setup that included gun, target array, pyrometer heads, oscilloscope with camera, velocity screens and electronic timer, camera, and flash X-ray, as shown in Figures 8 through 11.

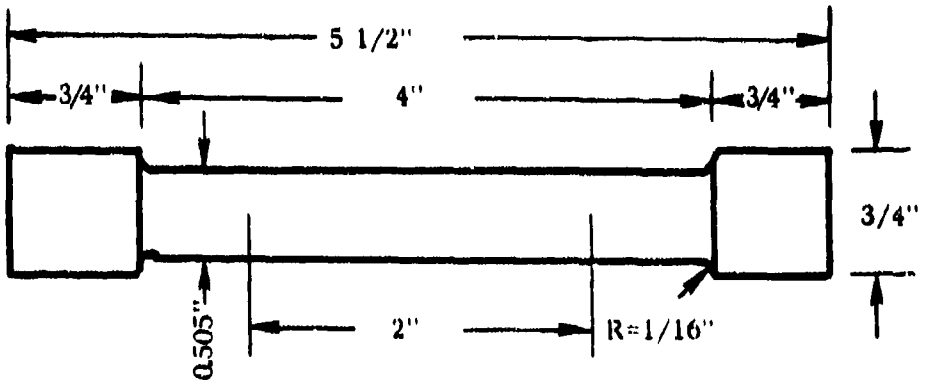

Figure 4. Standard .505 Inch Tensile Specimen

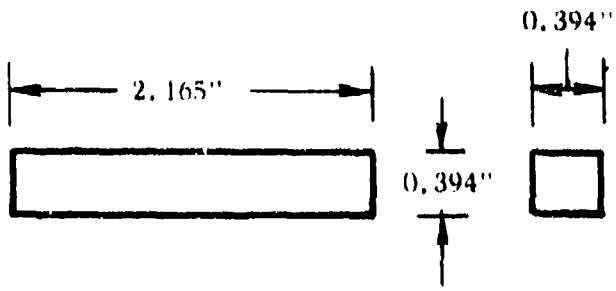

Figure 5. Charpy Unnotched Impact Specimen

TABLE II. PHYSICAL PROPERTIES OF MATERIALS EVALUATED

Alloy No.	Composition	Mod. of Elast. (10^6 psi)	Yield Str. (10^3 psi)	Ult. Str. (10^3 psi)	Elongation (%)	Red. of Area (%)	Hardness R_b	Unnotched Charpy Impact ft/lb *	Alloy Density g/cm^3	Fabricability at 750°F
1	MRE**	2.3	14.0	18.7	7.5	1.1	5	19.0	6.552	~50% reduction
		4.6	18.3	23.1	10.0	<1.0				before cracking
2	Cerium 90-95%	4.7	13.5	15.9	2.5	<1.0	3	4.5	6.689	~50% reduction
		4.2	13.5	18.1	2.5	<1.0				before cracking
3	MRE 6% Ni	5.7	----	13.2	0.048		65	no spec.	6.532	poor
		5.8	----	21.2	1.5	<1.0		(too brittle)		
4	MRE 10% Cu	4.8	----	13.5	0.14		42	1.5	6.656	poor
		4.5	----	11.8	1.5	<1.0				
5	MRE 7% Co	5.5	----	24.0	0.64		45	2.0	6.674	poor
		3.9	----		0	0				
6	MRE 15% Th	5.5	----	20.0	0.164		52	1.25	6.646	poor
		5.2	----	27.1	0					
7	Thorium	6.3	15.4	23.7	56.0	71.0	3	100+	11.564	
		5.9	15.4	23.3	53.0	70.5				
8	Uranium	13.2	24.9	58.9	2.0	5.0	65	26.5	18.979	
		20.1	27.7	48.8	1.0	5.5				
9	MRE 6% Ca	5.6	25.7	31.2	2.0	1.05	51	3.5	6.1952	poor
		5.4	27.7	32.1	1.0	1.8				

* Unnotched Charpy Impact Data: Impact Velocity - 11 ft/sec; Height of Drop - 1.88 ft; Wt. of Hammer - 53.2 lb

** MRE = Mixed Rare Earths

---- Data not obtained

TABLE II. PHYSICAL PROPERTIES OF MATERIALS EVALUATED (CONTINUED)

Alloy No.	Composition	Mod. of Elast. (10^6 psi)	Yield Str. (10^3 psi)	Ult. Str. (10^3 psi)	Elongation (%)	Red. of Area (%)	Hardness R_b	Unnotched Charpy Impact ft/lb*	Alloy Density g/cm^3	Fabricability at 750°F
10	MRE 4% In	4.9	21.6	27.9	>1.0	----	41	3.5	6.402	poor
		5.1	----	38.3	0.012					
11	MRE 3% Co-3% Fe	6.2	16.9	17.6	>1.0	----	29	2.0	6.706	poor
		5.9	----	11.5	0.02	----				
12	MRE 2% V	4.2	25.6	25.8	0.4	0.5	34	12.5	6.305	poor
		4.7	30.6	30.7	1.0	1.0				
13	MRE 13% Zn	5.6	----	20.8	0.016	0.5	75	1.5	6.4089	poor
		5.6	----	21.4	0.02	----				
14	MRE 10% Bi	5.0	----	----	0	----	38	2.0	6.5033	poor
		4.7	----	25.7	0.04	0.5				
15	MRE 2% Co-2% Ni - 2% Fe	4.7	----	11.5	0	----	68	1.5	6.6653	poor
		4.8	----	18.9	0.172	----				
16	MRE 50% Pb	Brittle Alloy - could not machine test specimens					27	no spec.	no spec.	poor
17	MRE 5% Mn	4.6	23.4	27.5	>1.0	0.5	39	2.5	6.5892	poor
		4.8	----	18.6	0.088	0.5				
18	MRE 3% Sn	5.3	----	25.5	0	----	22	4.5	6.7026	poor
		4.9	31.5	32.2	0.28	----	R_e70			
19	MRE 5% Mg	5.3	----	17.1	0	----	0	5.0	6.403	poor
							R_e57			
20	MRE 2% Pb	5.56	----	25.8	----	----	R_f82	14.2	6.4954	Ignited
		9.51	----	25.3						

---- Data not obtained

TABLE II. PHYSICAL PROPERTIES OF MATERIALS EVALUATED (CONCLUDED)

Alloy No.	Composition	Mod. of Elast. (10^6 psi)	Yield Str. (10^3 psi)	Ult. Str. (10^3 psi)	Elongation (%)	Red. of Area (%)	Hardness R_b	Unnotched Charpy Impact ft/lb*	Alloy Density g/cm^3	Fabricability at 750 °F
21	MRE 50% Th	Burned on reheating for fabricability test.								
22	Commercial Zirconium	14.8 12.8	49.0 47.1	70.0 69.1	25.7 25.0	47.5 47.0	85			
23	MRE 32% Zn	Could not machine			----	----	95	----	6.29	
24	MRE 15% Pb	6.61 5.713	---- ----	27.0 28.2	---- ----	---- ----	R_f90 ----	4.0 ----	6.4879	poor
25	MRE 2% Co	4.67	17.9	18.9	0.8	1.3	R_f60	2.0	6.4126	Ignited
26	MRE 4.5% Zn	9.45 8.6	19.1 19.3	23.5 25.3	1.3 0.8	5.1 0.6	R_f70	2.0	6.4645	Ignited
27	Commercial Ti (No RE)	14.1 13.7	53.8 55.7	69.6 69.2	25.0 25.6	59.6 58.6	86	----	4.4689	excellent
28	MRE 4% Fe	4.48 ----	19.2 ----	21.5 12.8	3.0 ----	0.25 ----	R_f54	3.0	6.5403	50% red. - poor
29	MRE 4% Al	5.39 5.17	20.2 20.2	22.5 23.7	0.8 0.8	1.4 1.6	---- R_f80	---- 6.0	---- 6.3951	Ignited
30	MRE 8% Mn	----	----	21.2	----	----	R_f80	3.1	6.5214	50% red. - excellent
31	MRE 15% Pb - 3% Mg - 3% Al									
32	MRE 9% Mg						R_f59	5.1	6.5585	50% red. -excellent 75% red. -cracked

---- Data not obtained

TABLE III. RESULTS OF STATIC TESTS

No.	Composition	Mass* (grains)	Autoignition Temperature °C	Peak Temperature °C	Time of Burn** (min)
1.	Mixed Rare Earths	20.4	443	805	13
		20.2	475	825	13
2.	90% - 95% Cerium	21.2	490	710	22
		21.4	492	655	21
3.	94% MRE	24.1	418	720	20
	+ 6% Nickel	18.8	418	675	20
4.	90% MRE	20.1	483	807	11
	+10% Copper	20.4	467	825	10
5.	93% MRE	19.0	393	760	10
	+ 7% Cobalt	19.5	405	790	9
6.	85% MRE	20.4	520	802	17
	+15% Thorium	20.5	521	817	18
7.	Thorium	37.3	***	---	--
8.	Uranium	50.3	***	---	--
9.	94% MRE	18.8	540	840	16
	+ 6% Calcium	21.5	552	853	10
10.	96% MRE	21.6	660	1000	29
	+ 4% Indium	16.2	652	880	35
11.	94% MRE	19.5	418	723	13
	+ 3% Cobalt	20.6	443	715	16
	+ 3% Iron				
12.	98% MRE	21.9	523	810	21
	+ 2% Vanadium	18.6	540	802	21
13.	87% MRE	20.5	422	713	--
	+13% Zinc	20.5	418	680	11
14.	90% MRE	20.4	580****	690	28****
	+10% Bismuth	20.7	580****	635	33****
15.	94% MRE	20.7	445	805	8
	+ 2% Cobalt	21.8	460	848	10
	+ 2% Nickel				
	+ 2% Iron				

TABLE III. RESULTS OF STATIC TESTS (CONTINUED)

No.	Composition	Mass* (grains)	Autoignition Temperature °C	Peak Temperature °C	Time of Burn** (Min)
16.	50% MRE +50% Lead	29.5	***	---	--
17.	95% MRE + 5% Manganese	17.3 17.3	530 525	800 776	17 18
18.	97% MRE + 3% Tin	19.6 20.1	593 605	775 855	28 26
19.	95% MRE +15% Magnesium	18.7 19.1	478 478	732 770	-- 22
20.	98% MRE + 2% Lead	19.7 20.1	565 550	795 728	24 21
21.	50% MRE +50% Thorium	Combusts spontaneously			
22.	Zirconium	20.2	***	---	--
23.	68% MRE +32% Zinc	21.4	***	---	--
24.	85% MRE +15% Lead	18.9 19.8	572 575	783 787	26 25
25.	98% MRE + 2% Cobalt	20.1 19.6	440 430	820 930	11 11
26.	95.5% MRE + 4.5% Zinc	19.3 19.9	445 440	790 795	13 11
27.	Titanium	14.1	***	---	--
28.	96% MRE + 4% Iron	20.0 19.7	510 500	792 910	18 16
29.	96% MRE + 4% Aluminum	19.2 17.4	485 480	770 815	16 19
30.	92% MRE + 8% Manganese	18.8 19.3	510 510	800 820	17 17
31.	79% MRE +15% Lead + 3% Magnesium + 3% Aluminum	19.6	500	780	19

TABLE III. RESULTS OF STATIC TESTS (CONCLUDED)

No.	Composition	Mass* (grains)	Autoignition Temperature °C	Peak Temperature °C	Time of Burn** (min)
32.	91% MRE	17.3	480	1070	12
	+ 9% Magnesium	17.2	490	815	14
	Methonalloy	20.8	452	803	13

* 0.25 inch diameter by 0.25 inch long cylinder - mass varies with sample density.

** Defined as time from autoignition until specimen cools to 400°C.

*** Autoignition was not achieved. Sample was heated to a maximum of 1120°C.

**** Autoignition temperature and burn time approximate.

--- Data not obtained.

Alloy 29 - 96% MRE + 4% Aluminum

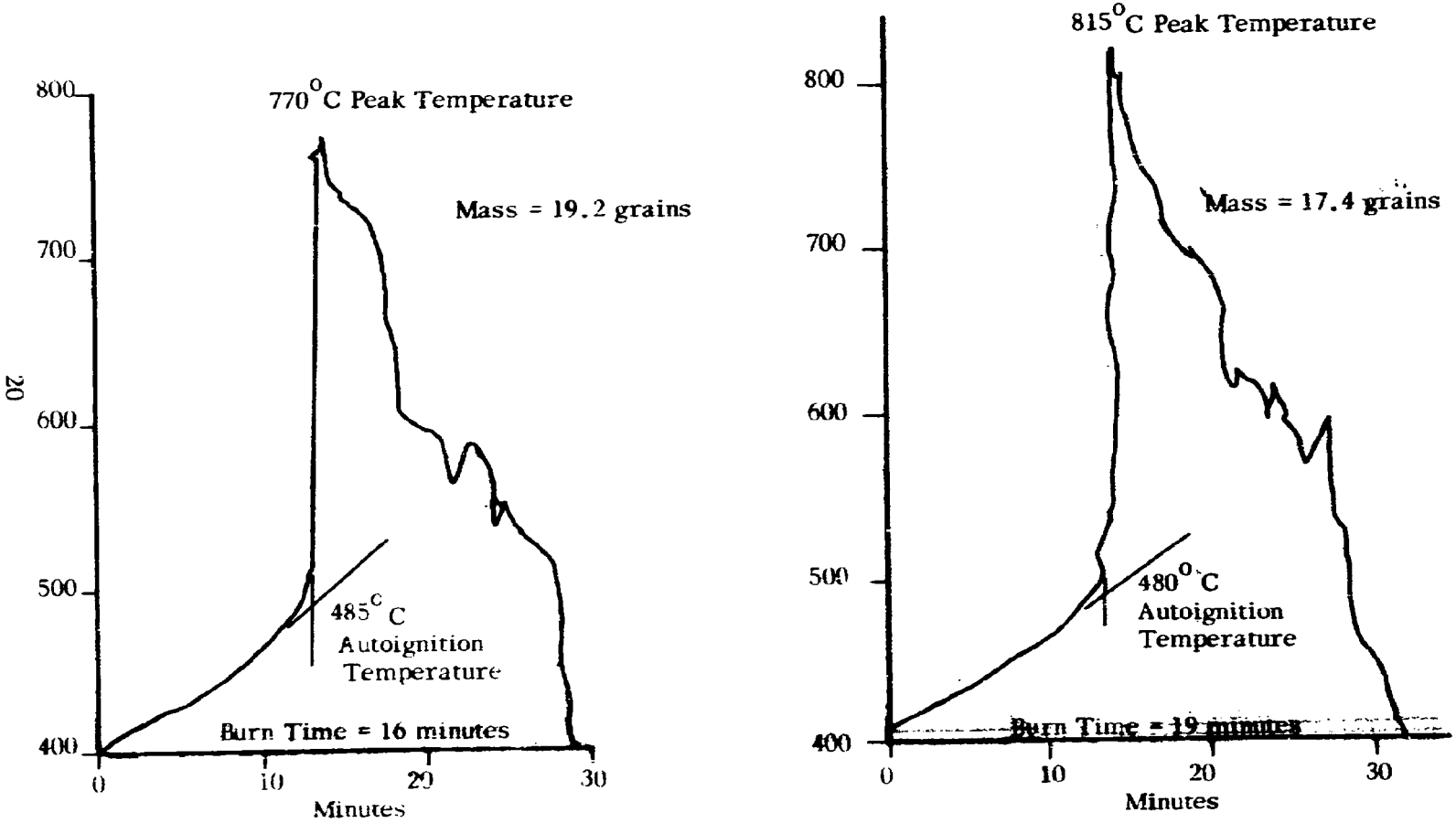

Figure 6. Time/Temperature Profile (Static)

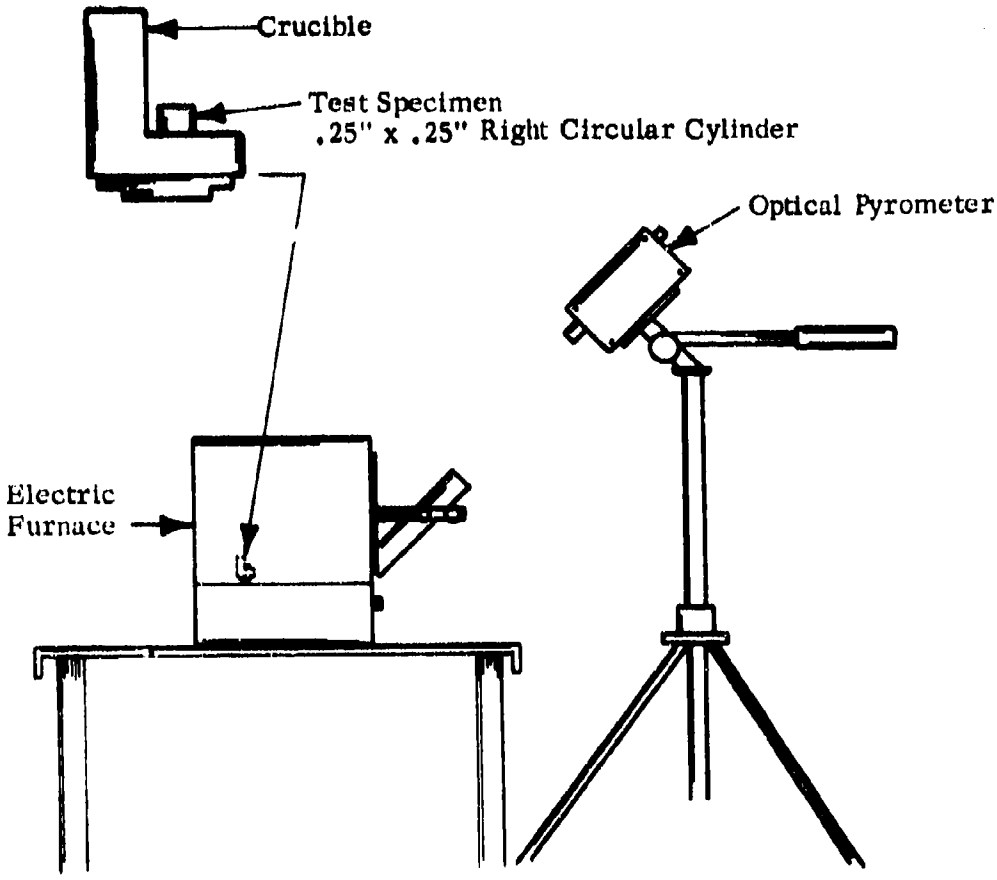

Figure 7. Thermal Test Setup (Static)

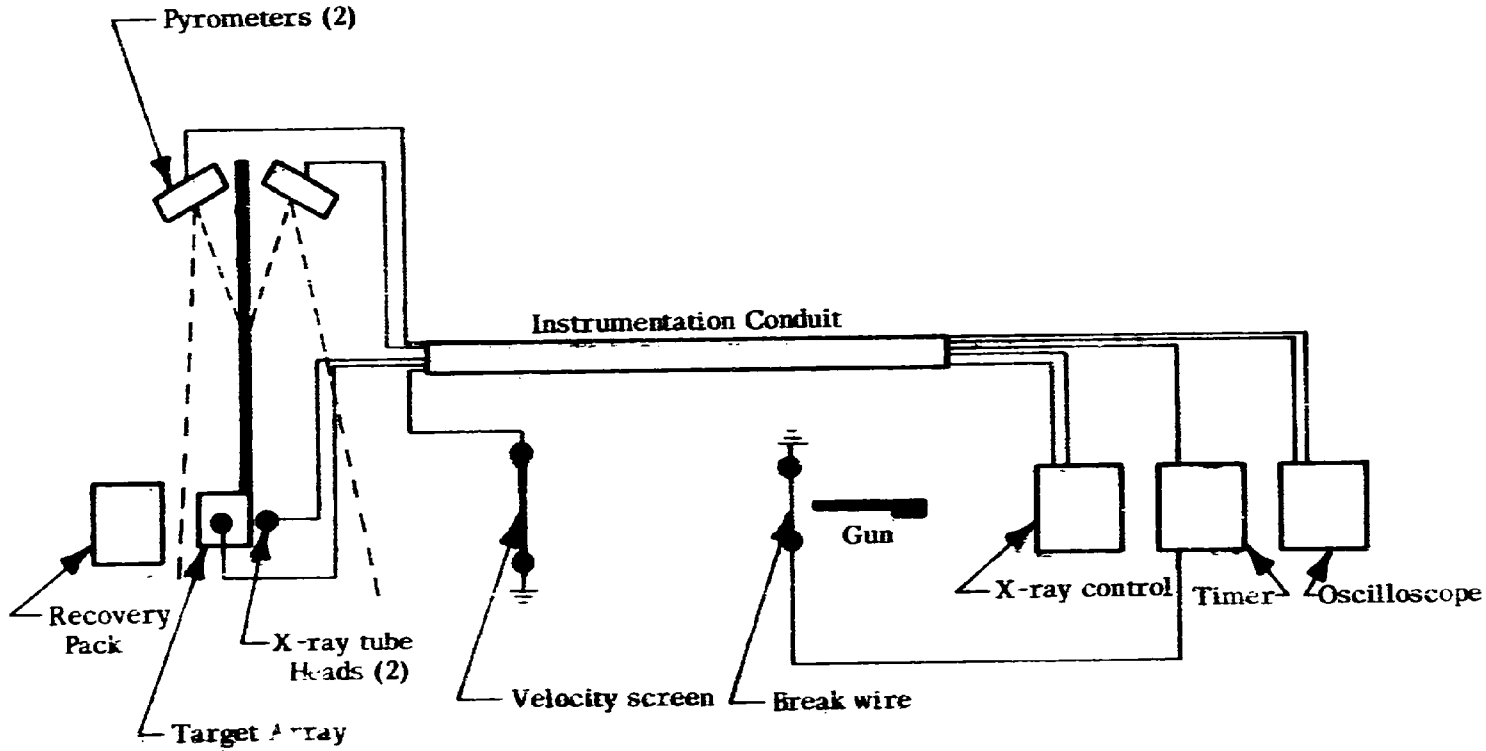

Figure 8. Instrumentation Schematic

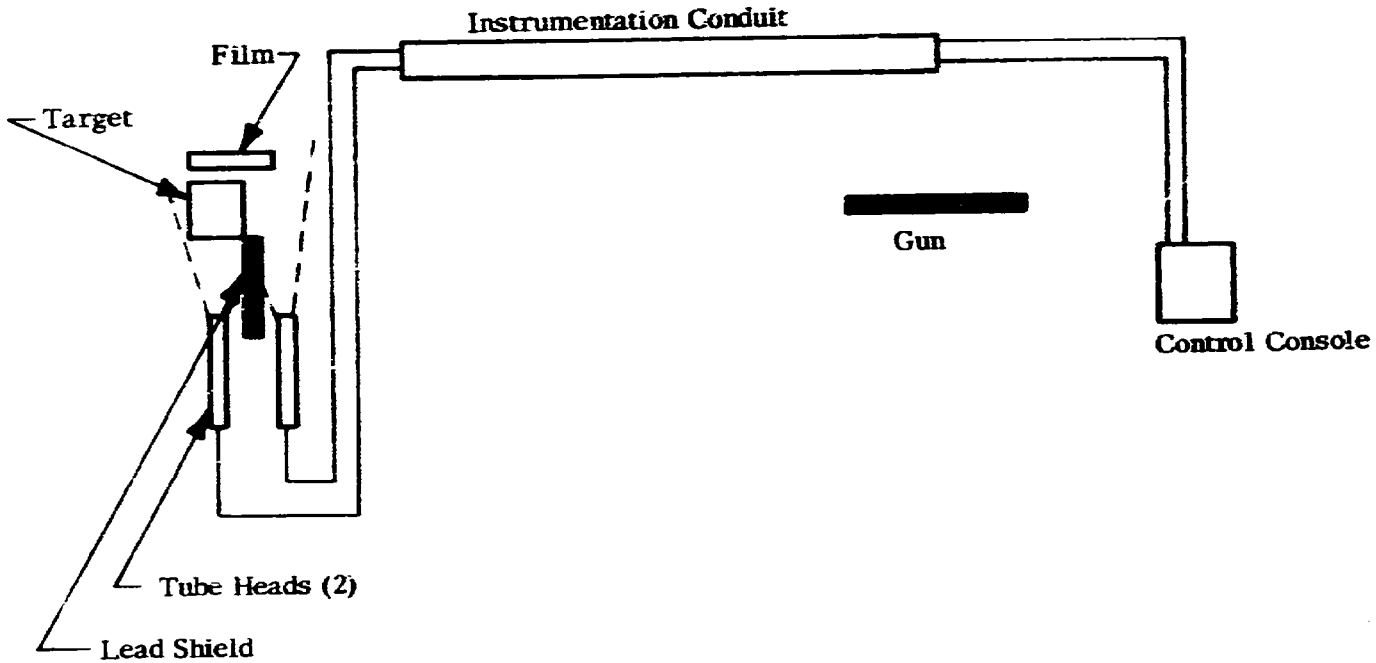

Figure 9. Flash X-Ray Schematic

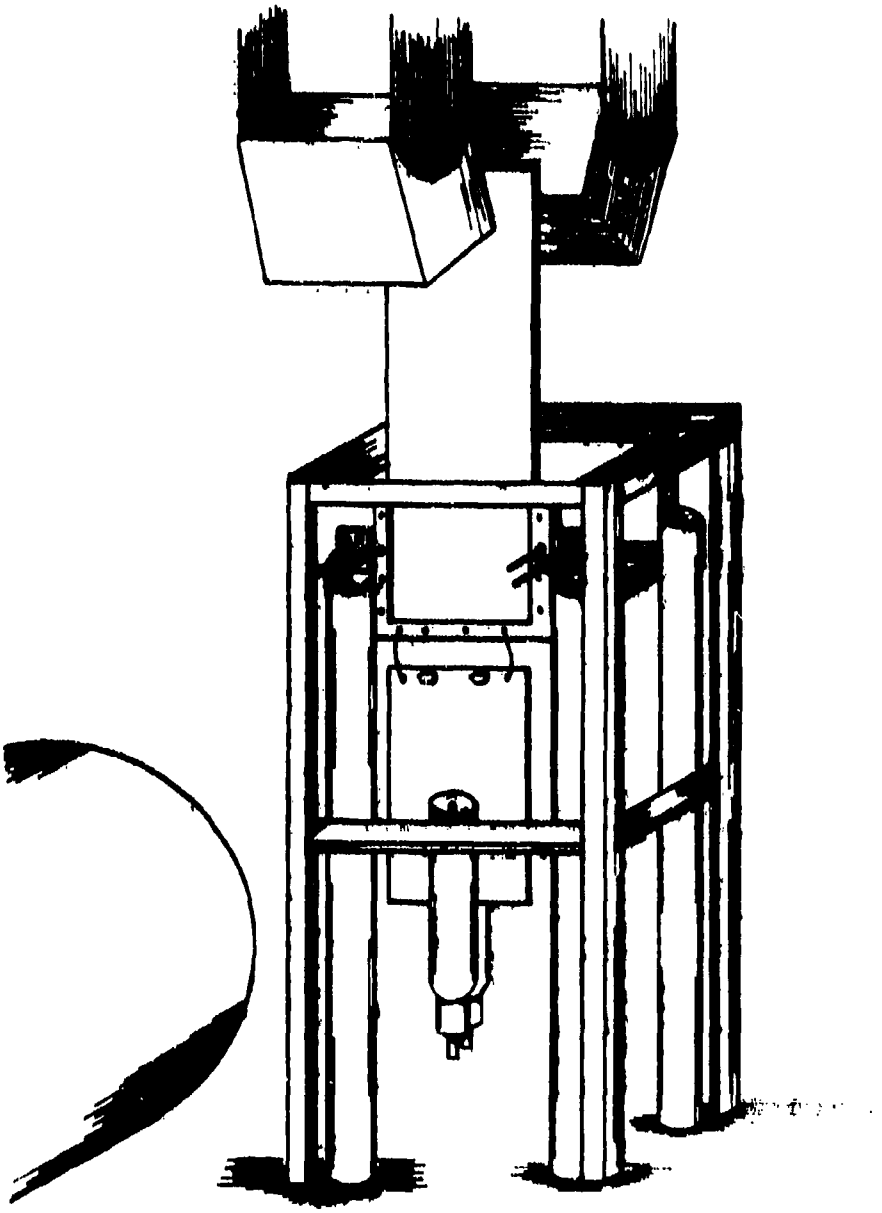

Figure 10. Target and Instrumentation Assemblies

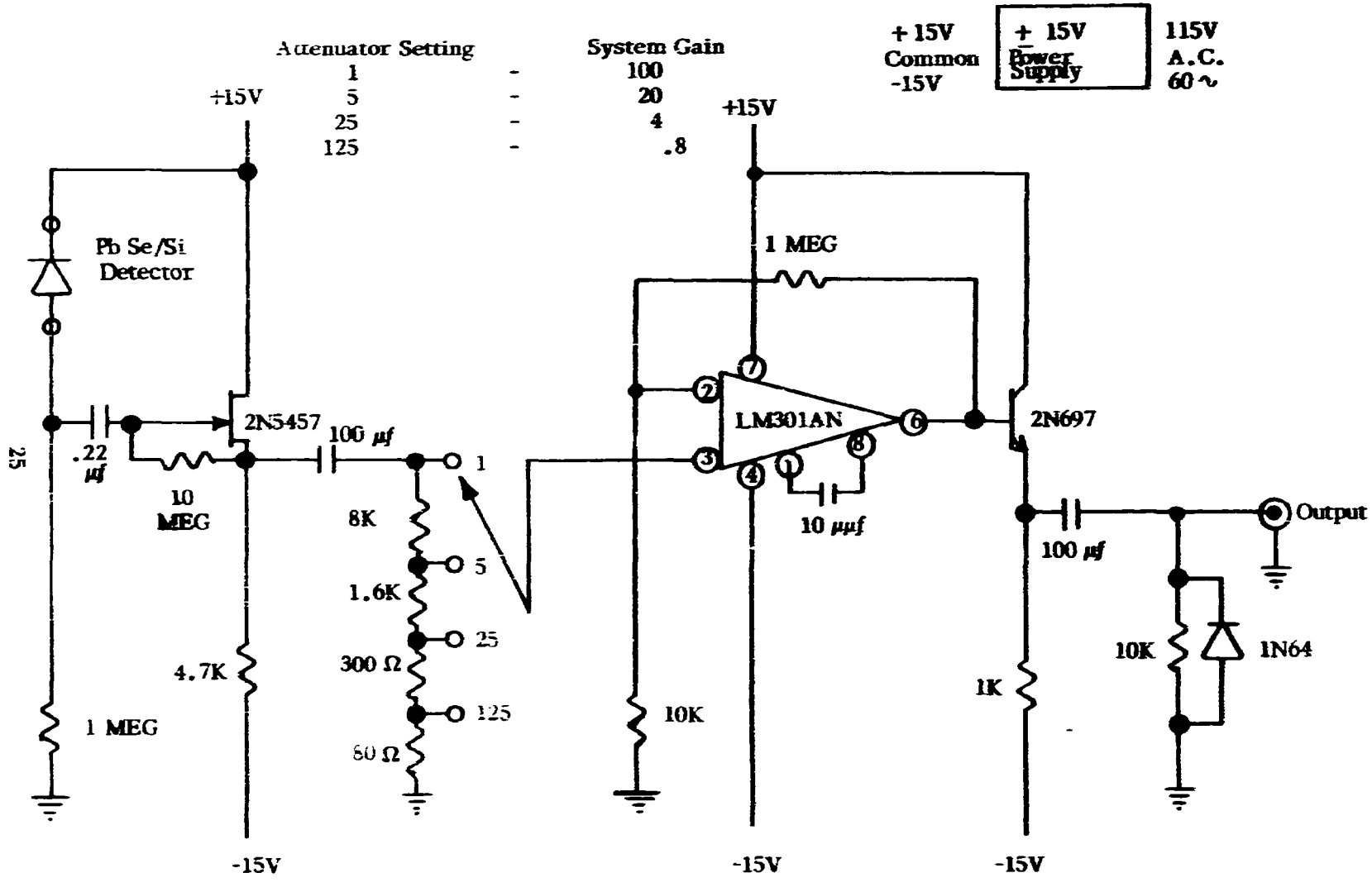

Figure 11. Impact Pyrometer Schematic

SECTION IV

APPARATUS AND INSTRUMENTATION

The projectile gun was a barrelled Mauser bolt action chambered for Caliber .30-'06 (Figure 12). The barrel was reamed to a smooth bore 0.308 inch diameter to accept a nylon-saboted projectile (Figure 13). Hercules Unique powder was found to be optimum for firing the 25-grain round (projectile plus sabot) over the desired velocity range.

The target array for the initial terminal effects testing consisted of the target plate holding assembly and the target plate. The holding assembly was constructed of two-inch galvanized pipe set in concrete, with a box framework of one-inch steel angle welded in place at the top. The target plates of steel, aluminum, or titanium were clamped to the front of the frame for each test.

The radiation pyrometers used in this program to measure heat flux on impact and penetration incorporated a silicon radiation detector AC-coupled to an amplifier powered by a 15-volt supply. This system was calibrated with the use of a quartz iodide source (ϵ =0.3) capable of temperatures up to 3000°C. This source and the pyrometers were placed the same distance apart as the instrument and the pyrophoric event would be during test, and the source was adjusted to a specific temperature. The voltage output of the pyrometer was then read and noted. This was done in increments of 100°C in the range between 1500°C and 2800°C. In this manner, source temperature detected as radiant power or intensity versus voltage output of the pyrometer was tabulated, and the results were graphed for calibration in terms of watt-seconds at the plane of projectile flight.

The pyrometers were connected to the vertical inputs of a dual-trace oscilloscope with Polaroid oscilloscope camera readout. The signal for triggering the sweep before the beginning of the event was the break circuit that also supplied the stop signal to the velocity counter/timer. The sweep speed and vertical sensitivity were set so as to keep the entire event within the range of the display, yet cover as much of the display as possible in order to obtain the best data precision. The resulting voltage versus time trace (Figure 14) was changed to thermal radiant power versus time table and numerically integrated to obtain total thermal energy output of the event. Over one thousand test firings were made during this program. The results from a portion of these tests were not reported because of data lost due to instrumentation instability.

A timer with break circuits (Figure 8) was used to determine the average velocity of the fragment over the twelve-foot range from the muzzle of the gun to impact. The unit has a resolution of ten μsec and was used exclusively in the μ sec range for maximum accuracy. The break element for start time was a nichrome wire placed one inch from the muzzle of the gun. The break element for stop time was printed circuit paper placed 9.625 feet downrange from the wire. Circuit elements were broken by the test projectile causing discharge of the respective circuit capacitors and the start and stop triggering of the electronic timer. Measurements taken by this method yield average velocity accuracy within 2 percent. Test velocities were reported to the nearest hundred feet per second.

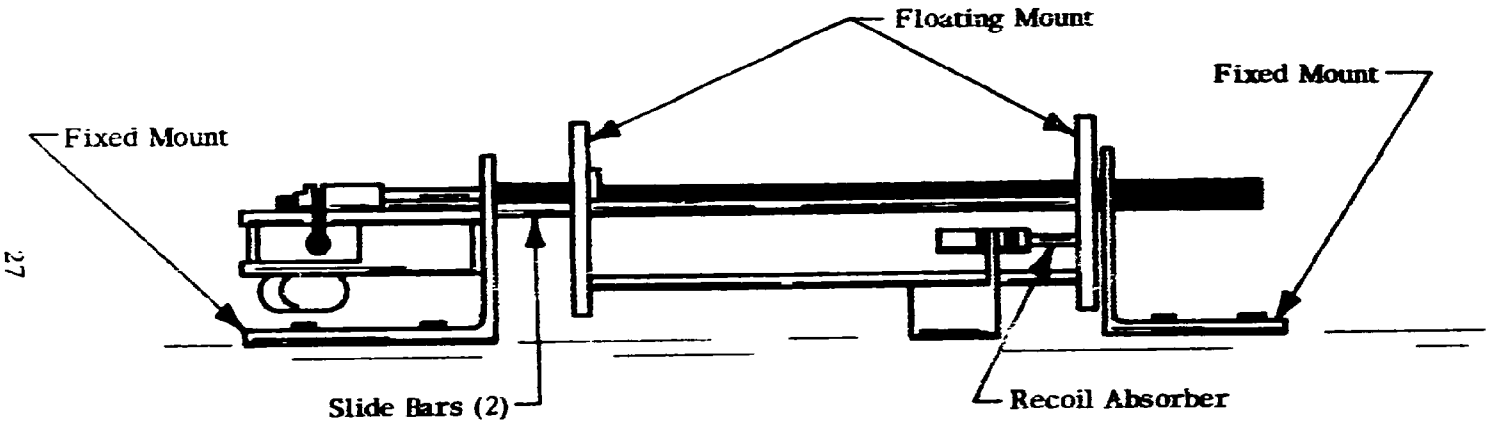

Figure 12. Projectile Gun and Mount

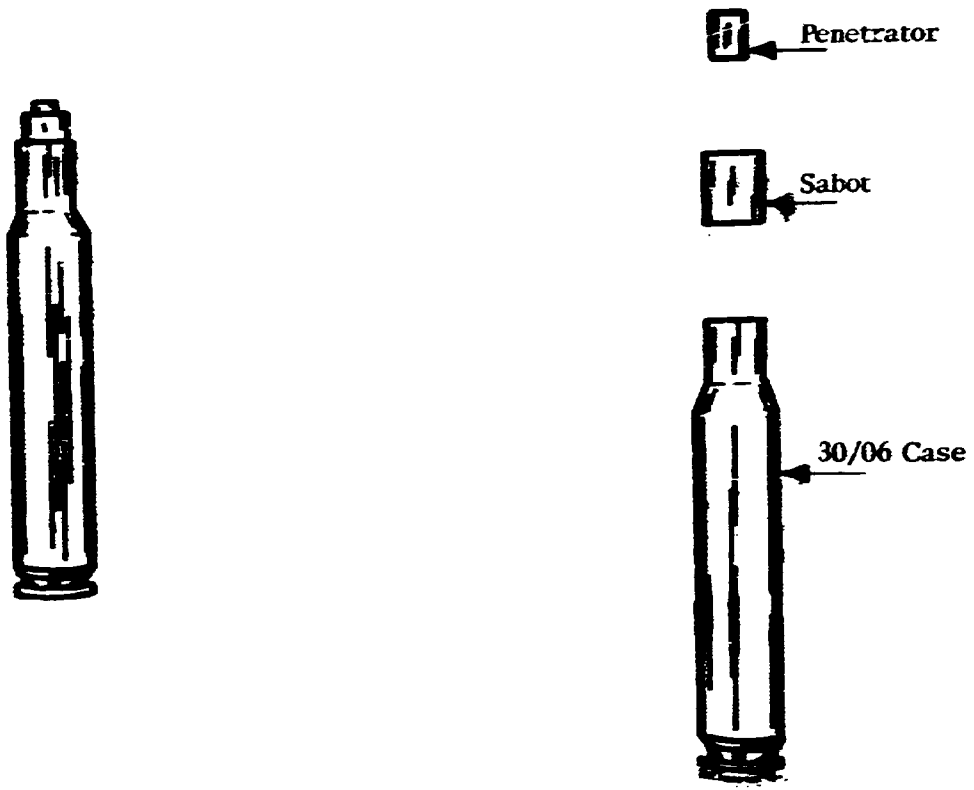

Figure 13. Cartridge Assembly

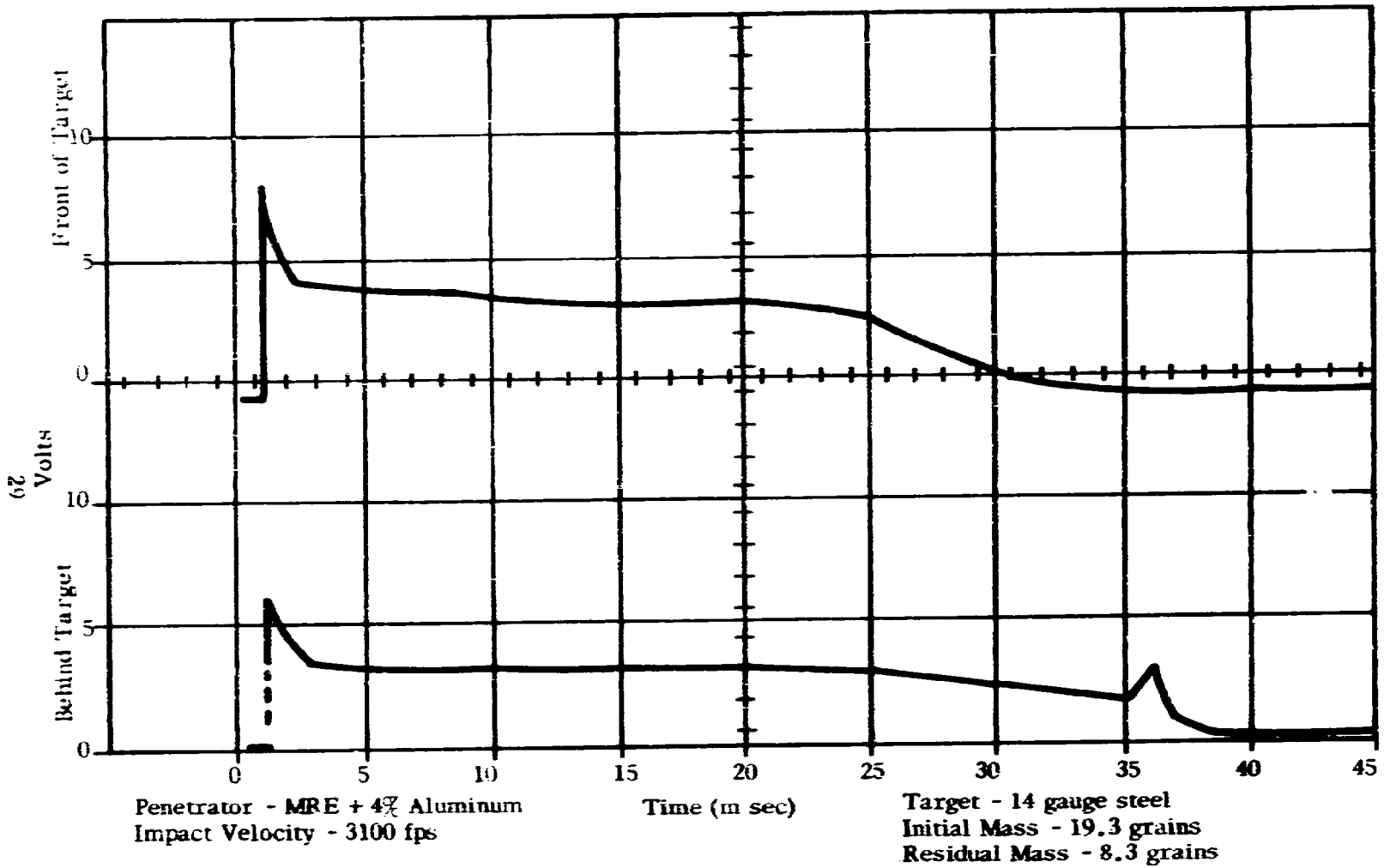

Figure 14. Oscilloscope Trace: Volts Versus Time

Open-shutter color photography was accomplished using a Polaroid camera placed on a tripod near the inside wall of the darkened target building. A small hole was drilled in the wall of the building and a cable release passed through from the camera to the outside. This arrangement permitted opening the shutter just before triggering the event and closing it immediately afterward. The resulting photographs were an excellent recording of the orientation and spatial distribution of the burning particles during the event.

The flash X-ray used in this program incorporated two pulsers, two tube heads, and two trigger amplifiers. The tube heads were placed approximately eight inches from the event position with both facing perpendicular to the flight path of the fragment. One head was two inches in front of the target plate; the second was four inches behind the target plate. The pulsers and the trigger amplifiers were in the control and firing area. The X-ray was triggered by a pulse from a break circuit incorporating a printed circuit paper break element. This element was placed in front of the target plate, triggering the primary amplifier just before fragment impact. The delayed trigger amplifier was preset to trigger after impact, so as to picture the fragment breakup and target spall. One sheet of 8 inch by 10 inch film was used for each shot and placed so that both the images were on the one sheet. By measuring the fragment displacement as pictured and using the preset delay time, an average residual or behind-the-plate velocity could be computed. The residual velocity values reported take into accoun' pulser head viewing parallax.

Instrumentation for the ignition and flammability tests was limited to velocity measurement and high speed motion picture coverage. Velocity measurement was accomplished by the breakwire/printed circuit paper method used in the terminal effects testing. Motion picture photography with a capability of 4000 frames/second was provided by a Hycam camera calibrated with a timing mark generator. From this motion picture coverage, additional data were obtained on pyrophoric persistence and fuel ignition delay after penetration.

SECTION V

EXPERIMENTAL RESULTS

Physical properties tests using standard ASTM metal testing techniques and equipment were accomplished on twenty-seven MRE (mixed rare earths) alloys and five pure metals. The results are presented in Table II. The properties reported include hardness, yield strength, ultimate strength, modulus of elasticity, elongation, reduction of area, and impact toughness. Pure cerium and MRE in the as-cast condition brittle-fracture in tension with their elongation and reduction of area at ultimate yield being small values. Alloying of the MRE enhances this brittleness to the point that all tensile failures are in the brittle mode, usually at the shoulder, with no elongation or necking of the tensile specimen. Hardness of the mixed rare earths is 5 and that of 90-95% cerium is 3 on the Rockwell B scale; alloying generally results in a harder material. Three exceptions are the alloy of MRE + 4% iron, MRE + 2% cobalt, and the magnesium alloys tested. The impact toughness of pure cerium is 4.5 on the Charpy unnotched test, a low value, while the MRE value is 19.0. Further alloying of the MRE caused a decrease in impact resistance. The ultimate strength of all the MRE alloys is low compared to common structural metals.

Figure 6 is representative of the time-temperature profiles for all materials tested; Table III is a summary of the autoignition temperatures, peak temperatures, and burn time. For these tests, the time of burn was defined as the time from autoignition until the specimen cooled to 400°C. In some cases, autoignition could not be achieved with the furnace and other means were used to elevate the specimen temperature to a maximum of 1120°C. In no case was sustained burning of the specimen achieved by this method. The specimens that could not be ignited were the pure metals zirconium, thorium, titanium, uranium, and zirconium-tin and the alloys MRE +50% lead and MRE +32% zinc. Alloy 14 (90% MRE + 10% bismuth) did not show a rapid rise in temperature after ignition, and therefore autoignition temperature was not readily discernible. The temperature listed in the table for this alloy is approximate, as are the burn times.

A survey of the terminal effects of thirty-two metals and alloys against 14-gauge (0.074-inch) steel sheet was conducted and is summarized in Table IV. The velocity regime for this survey ranged from 1500 feet per second to 3000 feet per second. The test velocities recorded were rounded to the nearest 100 feet per second. Three general conclusions can be drawn from the results of this survey. First, the ballistic limit is approximately 1900 feet per second velocity with a 20.5-grain pyrophoric penetrator against this target. Second, the variation of apparent peak temperature over all shots (except the titanium projectile) was very small (2400°C to 2700°C), with the majority falling in the 2500°C to 2600°C range. Third, despite this very small peak temperature spread, the total thermal energy range was considerable. This was due to the length of the event duration which is in proportion to the total thermal energy output.

Upon completion of these screening tests, five of the thirty-two pyrophoric compositions were selected for detailed testing and analysis. The compositions elected were chosen with the concurrence of the sponsor. Prime

TABLE IV. DYNAMIC TEST RESULTS

No.	Composition	Velocity (fps)	Thermal Energy (watt-sec/m^2)		Event Duration (milliseconds)		Peak Temperature (°C)		Mass (grams)	
			Front of Plate	Back of Plate	Front of Plate	Back of Plate	Front of Plate	Back of Plate	Initial	Residual
1	Mixed Rare Earths	1500	4,400	*	8	*	2500	*	19.7	*
		1800	5,500	*	8	*	2600	*	20.0	*
		2800	9,400	4,700	8.5	7	2600	2600	20.5	7.2
		3000	3,600	3,400	5.5	5.5	2600	2500	20.5	14.6
2	90%-95% Cerium	1700	13,300	*	13	*	2600	*	21.3	*
		1900	5,500	3,700	7.5	6.5	2700	2500	21.5	15.9
		2500	10,400	4,700	13	7.5	2500	2400	21.1	16.2
		2900	7,800	4,000	9.5	6.5	2600	2400	19.1	12.2
3	94% MRE + 6% Nickel	1600	7,600	*	10	*	2700	*	20.8	*
		1800	9,900	*	12.5	*	2700	*	20.4	*
		2500	13,300	6,200	17	8.5	2600	2600	21.3	15.2
		2900	7,100	5,400	10	7	2600	2500	21.3	11.1
4	90% MRE + 10% Copper	1700	7,800	*	10	*	2600	*	20.7	*
		1900	7,600	4,200	10	6.5	2700	2500	21.1	--
		2500	5,600	4,400	8	6.5	2600	2500	21.0	4.2
		2800	4,100	5,300	6.5	7.5	2600	2600	20.6	4.5
5	93% MRE + 7% Cobalt	1500	8,600	*	10	*	2600	*	20.7	*
		1800	10,800	*	14.5	*	2700	*	20.3	*
		2200	8,700	3,900	12	6.5	2600	2500	20.6	15.6
		2600	6,800	5,700	9.5	8	2600	2600	20.9	12.6
6	85% MRE + 15% Thorium	1500	4,500	*	8	*	2600	*	20.7	*
		1700	5,300	*	8	*	2700	*	20.7	*
		2300	7,400	3,000	10	5.5	2600	2500	19.5	16.5
		2700	6,100	2,800	8.5	5	2600	2500	20.0	12.9

TABLE IV. DYNAMIC TEST RESULTS (CONTINUED)

No.	Composition	Velocity (fps)	Thermal Energy (watt-sec/m^2)		Event Duration (milliseconds)		Peak Temperature (°C)		Mass (grains)	
			Front of Plate	Back of Plate	Front of Plate	Back of Plate	Front of Plate	Back of Plate	Initial	Residual
7	Thorium	2300	1,000	700	3	2.5	2500	2500	37.5	35.3
		2400	1,400	1,400	3	3.5	2400	2500	36.1	32.9
		3000	950	980	3	3	2400	2500	36.1	32.0
8	Uranium	2400	2,500	3,300	4.5	5	2500	2500	50.4	--
		2800	2,400	2,500	5	4.5	2500	2500	56.0	--
9	94% MRE +	1500	7,800	*	12	*	2500	*	19.3	*
	6% Calcium	2400	7,400	2,800	10	5	2600	2500	19.5	17.2
		2600	6,000	4,900	8.5	7	2600	2600	19.9	16.7
10	96% MRE +	1700	7,000	*	10	*	2600	*	20.8	*
	4% Indium	1900	8,900	*	12	*	2700	*	20.8	*
		2300	5,700	3,300	8.5	5.5	2500	2500	19.4	15.3
		2800	4,600	2,700	7	5	2500	2500	20.4	14.6
11	94% MRE +	1900	9,200	5,200	12.5	8.5	2600	2600	21.9	11.9
	3% Cobalt	2200	12,900	3,300	16	5.5	2600	2500	20.2	17.3
	+3% Iron	2800	9,600	3,300	9.5	6	2600	2700	21.4	13.3
12	98% MRE +	1700	7,000	*	10.5	*	2600	*	20.1	*
	2% Vanadium	2100	10,000	3,000	12.5	5.5	2700	2500	19.3	15.9
		2300	7,600	2,700	10	4.5	2600	2500	20.9	17.0
		2900	3,100	2,600	5	5	2600	2500	20.4	14.9
13	87% MRE +	1600	7,600	*	6.5	*	2600	*	20.5	*
	13% Zinc	1800	5,100	*	7.5	*	2600	*	20.2	*
		2400	5,200	3,300	7.5	5.5	2700	2500	20.4	0
		3000	4,400	4,300	6.5	6.5	2600	2600	20.6	6.0

TABLE IV. DYNAMIC TEST RESULTS (CONTINUED)

No.	Composition	Velocity (fps)	Thermal Energy (watt-sec/m^2)		Event Duration (milliseconds)		Peak Temperature (°C)		Mass (grains)	
			Front of Plate	Back of Plate	Front of Plate	Back of Plate	Front of Plate	Back of Plate	Initial	Residual
14	90% MRE + 10% Bismuth	1600	5,200	*	8.5	*	2600	*	20.8	*
		1700	7,800	*	6.5	*	2500	*	20.6	*
		2600	6,700	3,200	9.5	6	2600	2500	21.7	14
		2700	4,900	2,300	7.5	4.5	2500	2400	20.8	15.3
15	94% MRE + 2% Cobalt +2% Nickel +2% Iron	2200	8,000	5,200	10.5	6	2600	2400	21.1	15.7
		2300	7,800	5,400	10	7	2600	2500	21	14.1
		2900	5,100	2,300	7	3.5	2600	2500	21.2	17
16	50% MRE + 50% Lead	2900	5,700	5,000	7.5	7	2500	2500	28.2	1.3
		3300	5,200	4,700	7.5	7	2500	2500	29.4	0
17	95% MRE + 5% Manganese	2000	6,800	2,600	9	4.5	2600	2500	21.2	16.6
		2300	6,500	2,900	9	4.5	2600	2500	20.4	17.2
		2600	4,600	3,700	7	5.5	2500	2400	20.7	15
		2700	3,900	2,500	5.5	4	2500	2400	21	16.3
18	97% MRE + 3% Tin	1500	15,700	*	18	*	2600	*	20.0	*
		1800	14,600	*	16.5	*	2700	*	19.6	*
		2300	15,600	2,700	17.5	3	2500	2500	20.1	15.9
		2800	9,600	2,900	12	3.5	2600	2400	19.5	15.4
19	95% MRE + 5% Magnesium	2600	4,500	3,000	7	4.5	2600	2500	20.1	15.9
		2700	6,800	3,200	9	5	2500	2400	20.7	15
20	98% MRE + 2% Lead	1600	13,700	*	19	*	2600	*	20.3	*
		1800	13,700	*	19	*	2600	*	19.8	*
		2200	9,600	3,000	12.5	5	2600	2400	19.7	16.8
		2500	9,600	3,400	13.5	5	2600	2500	20.2	16.3

TABLE IV. DYNAMIC TEST RESULTS (CONTINUED)

No.	Composition	Velocity (fps)	Thermal Energy (watt-sec/m^2)		Event Duration (milliseconds)		Peak Temperature (^{o}C)		Mass (grains)	
			Front of Plate	Back of Plate	Front of Plate	Back of Plate	Front of Plate	Back of Plate	Initial	Residual
21	50% MRE + 50% Thorium	Combusts Spontaneously								
22	Zirconium	2100	3,200	3,000	5	5	2500	2300	20.1	19.1
		2200	2,500	3,300	5	5.5	2600	2500	20.4	19.2
23	68% MRE + 32% Zinc	1800	37,000	*	44.5	*	2600	*	19.8	0
		2800	5,100	3,700	6.5	5	2600	2500	27.4	0
		2900	7,700	7,900	8.5	9.5	2600	2500	21.3	0
24	85% MRE + 15% Lead	1700	17,700	*	23	*	2600	*	19.4	*
		2200	19,700	3,800	26.5	5.5	2600	2400	19.7	17.2
		2400	14,300	3,200	19	5	2600	2400	19.8	17.7
25	98% MPE + 2% Cobalt	1600	19,000	*	23.5	*	2600	*	19.6	*
		1800	13,700	*	16.5	*	2700	*	19.9	*
		2400	17,500	5,600	21	7.5	2600	2400	19.2	14.6
		2800	10,500	3,700	12	4.5	2600	2400	20.0	10.6
26	95.5% MRE + 4.5% Zinc	1500	21,100	*	25.5	*	2600	*	19.7	*
		1800	10,400	*	12.5	*	2600	*	20.0	*
		2300	25,900	5,400	30	6.5	2600	2400	20.2	17.5
		2800	9,900	4,000	12	4.5	2500	2400	19.7	17.0
27	Titanium	2100	800	*	3	*	2400	*	13.5	*
		2600	826	1,700	3	4	2400	2400	14.5	13.3
		3000	1,200	1,800	4	4	2300	2400	13.5	12.4

TABLE IV. DYNAMIC TEST RESULTS (CONCLUDED)

No.	Composition	Velocity (fps)	Thermal Energy (watt-sec/in^2)		Event Duration (milliseconds)		Peak Temperature (^{o}C)		Mass (grains)	
			Front of Plate	Back of Plate	Front of Plate	Back of Plate	Front of Plate	Back of Plate	Initial	Residual
28	96% MRE + 4% Iron	1600	16,500	*	15.5	*	2600	*	20.0	*
		1800	9,700	*	12.5	*	2700	*	19.8	*
		2200	11,900	3,500	15.5	5.5	2600	2500	20.1	17.4
		2800	7,200	2,500	10	4.5	2600	2500	20.0	4.0
29	96% MRE + 4% Aluminum	1400	6,800	*	10.5	*	2600	*	19.6	*
		1600	6,800	*	10.5	*	2600	*	19.4	*
		2300	7,800	3,800	10.5	6	2600	2500	19.7	16.3
		2800	5,400	3,600	8	6	2600	2500	19.6	15.7
30	92% MRE + 8% Manganese	1400	4,400	*	7.5	*	2600	*	19.4	*
		1800	7,600	*	10.5	*	2600	*	19.5	*
		2400	9,200	2,000	13	4	2600	2500	19.9	16.9
		2800	5,800	2,700	8.5	4.5	2600	2600	20.0	12.8
31	79% MRE + 15% Lead + 3% Magnesium + 3% Aluminum	2200	9,700	2,300	12.5	3.5	2600	2500	18.9	15.8
		2300	8,500	3,200	10.5	4.5	2600	2600	19.4	16.4
		2600	6,700	2,200	8.5	3.5	2600	2500	19.4	17.0
32	91% MRE + 9% Magnesium	1500	7,500	*	11.5	*	2600	*	20.1	*
		1900	7,600	*	11	*	2600	*	20.5	*
		2400	9,200	2,400	12.5	4.5	2600	2400	20.1	17.4
		2900	4,300	2,700	6.5	5	2600	2500	20.7	11.7
	Methonalloy	2200	5,300	1,900	8	4	2600	2600	19.3	15.6
		2300	8,600	2,300	11	3	2600	2500	19.3	16.2
		2900	5,500	2,300	8	3.5	2500	2400	19.4	14.3

*Projectile did not penetrate target.
--Data not obtained.

considerations for selecting the five candidate materials for further testing were:

1. Storability (stability in air)
2. Ignition pulse duration
3. Large residual mass

In addition, limited testing was conducted with a 20-grain (0.180 by 0.180 right circular cylinder) depleted uranium penetrator.

Stability in air was considered a basic criterion to allow for ease of fabrication and storage of any possible munition incorporating these metals. A qualitative survey of the oxidation rates was conducted (Table I). All of the pure metals except cerium and the mixed rare earths were relatively stable in air with zirconium and titanium exhibiting no noticeable oxidations and with uranium and thorium showing a tightly adhering protective oxide. For the purposes of this program, only those materials showing stability in air were considered for further testing. It should be noted, however, that some otherwise promising materials have been discarded by this procedure.

Due to the uniformity of densities throughout the various alloys, penetrability is largely a function of projectile velocity and therefore was not a great factor in selection.

Large residual mass was considered a necessity for secondary penetration to any flammables such as fuel, hydraulic fluid, etc. Also, the time length of the pyrophoric event after impact was added as a necessary requirement due to the delays encountered before a flammable fuel/air ratio is formed. Machinability of the materials was considered also but was not a prime factor, as only alloys 16 and 23 presented any great problem and were immediately discarded as being too brittle to be of any practical use. Using these factors alloys 14 (90% MRE + 10% bismuth), 19 (95% MRE + 5% magnesium), and 29 (96% MRE + 4% aluminum) were chosen for final testing plus zirconium and zirconium-tin as required by contract amendment.

Final terminal effects testing was conducted on these materials using target plates of steel, aluminum, and titanium, and at velocities ranging from 1500 feet per second to 5000 feet per second (Tables V through X). As an overall conclusion, it can be seen that the mixed rare earth alloys yield greater thermal output at lower impact velocities than zirconium and zirconium-tin. At velocities above 3000 to 3500 feet per second (depending on the composition), the mixed rare earth alloys begin to break up into numerous particles while zirconium and zirconium-tin are good penetrators but have just begun to yield pyrophoric action. This result could have been expected from the physical properties data, which showed that the MRE alloys are extremely brittle while zirconium is more ductile. This brittleness leads to brittle failure and breakup at low impact velocities and some resulting intergranular friction which results in good pyrophoric output. Zirconium, on the other hand, deforms at low impact velocities and therefore has only attrition action at the target/projectile interface. At the higher impact velocities, the MRE brittleness causes excessive fragmenting and a subsequent loss in residual mass, while zirconium begins to break up rather than simply being deformed.

Figures 15 through 32 are least square exponential fit graphs of the data of Tables V through XVI. The relationship between the pyrophoric thermal energy in front of and behind the plate is plotted as a function of projectile velocity. In all cases there is a velocity above which the thermal effects behind the plate equal and exceed the front-of-the-plate effects. A considerable variation between materials is apparent.

Incendiary testing of the chosen alloys was conducted on a simulated truck fuel tank (Figure 33) and a simulated aircraft wing fuel tank (Figure 34 and 35). The flammable liquids used were Mogas and kerosene (flash point approximately 135°C) and the impact plates were 0.050-inch aluminum and 0.074-inch mild steel. The initial impact velocity used against the wing tanks was 3000 feet per second for a series of three shots. The initial velocity against the truck tank was in the 1800 feet per second range, which was close to ballistic limit. If a fire was initiated, the next series of three test shots would be 500 feet per second lower. The highest velocity used for this testing was 3500 feet per second, while the lowest was in the 1000 feet per second range. Results of this testing are given in Tables XVII through XX.

The MRE alloys are better fire starters than the zirconium or zirconium-tin fragments. This probably due to better fragment break-up and longer particle burning time of the MRE. Zirconium and its alloys do not break up well against medium or soft targets at the lower velocities (3000 feet per second or lower). Another factor is the lack of persistence of the burning zirconium particles at the lower velocities.

No fires were started with kerosene as the flammable liquid. This is probably due to the high flash point (136°F). As is shown in the tabulation below, this flash point does conform very closely with diesel fuel and JP-5 but is not at all similar to JP-4.

Fuel	Flash Point (°F)
Test Kerosene	135 through 137
Diesel	100 through 130
JP-5	95 through 145
JP-4	-10 through 30
Mogas	-36 through -45

A few test shots were conducted to simulate a multiple plate target. In these tests two 0.074-inch thick mild steel plates were placed 6 inches apart and the projectile fired through the plate at a selected test velocity. The residual particles were recovered in stacked Celotex® ceiling tiles. The results of these tests are presented in Table XXI.

TABLE V. TERMINAL EFFECTS ALLOY 14 (MRE + 10% BISMUTH)

Velocity (fps)		Thermal Energy (watt-sec/m^2)		Event Duration (milliseconds)		Peak Temperature (°C)		Mass (grains)	
Initial	Residual*	Front	Back	Front	Back	Front	Back	Initial	Residual
Steel Target Plate									
1600	---	5,200	**	8.5	**	2600	**	20.8	**
1700	---	7,800	**	6.5	**	2500	**	20.6	**
2100	700	5,500	6,100	5.0	9.5	2700	2300	21.9	14.5
2600	---	6,700	3,200	9.5	6.0	2600	2500	21.7	14.0
2600	---	4,900	2,300	7.5	4.5	2500	2400	20.8	15.3
3000	1100	3,800	8,800	4.0	12.0	2700	2400	20.8	12.2
4200	1600	7,800	12,000	8.0	12.0	2700	2700	22.2	0.6
Titanium Target Plate									
2000	900	20,100	14,400	30.0	24.5	2700	2400	22.1	15.3
2800	---	7,400	4,000	8.5	5.0	2700	2700	20.8	13.9
2900	1100	8,600	6,000	10.0	8.0	2600	2400	20.6	7.7
4000	---	3,800	44,100	4.0	49.0	2700	>2800	20.0	3.3
4000	1500	13,600	37,200	17.0	51.0	2600	>2800	17.8	1.8
4900	---	4,000	77,400	4.0	81.0	2700	>2800	21.6	3.8
5000	---	1,900	52,500	2.0	>50.0	2700	>2800	20.8	4.2

* Determined from flash X-ray.

** Projectile did not penetrate target.

--- Data not obtained.

TABLE V. TERMINAL EFFECTS ALLOY 14 (MRE + 10% BISMUTH) (CONCLUDED)

Aluminum Target Plate

Velocity (fps)		Thermal Energy (watt-sec/m^2)		Event Duration (milliseconds)		Peak Temperature (°C)		Mass (grains)	
Initial	Residual*	Front	Back	Front	Back	Front	Back	Initial	Residual
2500	900	3,200	1,700	5.0	3.0	2600	2500	21.0	15.0
2600	1100	2,800	1,100	4.0	2.0	2600	2600	20.9	17.2
2700	---	1,800	1,800	2.5	2.5	2700	2600	20.4	13.1
3000	1300	2,500	1,800	4.0	2.0	2600	2700	20.4	9.6
3000	1300	1,700	14,400	3.0	19.5	2600	2800	20.7	7.8
3500	1500	2,000	2,600	3.0	3.0	2700	>2800	19.1	---
3600	1500	4,500	26,900	7.0	30.0	2700	>2800	21.0	0.6
4000	---	3,000	23,500	4.0	29.0	2700	>2800	19.6	4.2
4200	---	2,100	43,100	3.0	>45.0	2700	>2800	19.5	1.2
5000	---	3,100	46,500	3.0	>45.0	2700	>2800	20.5	1.8
5100	---	3,600	87,800	4.0	>90	2700	>2800	20.4	1.2

*Determined from flash X-ray.

--- Data not obtained.

TABLE VI. TERMINAL EFFECTS ALLOY 19 (MRE + 5% MAGNESIUM)

Velocity (fps)		Thermal Energy (watt-sec/m^2)		Event Duration (milliseconds)		Peak Temperature (^{o}C)		Mass (grains)	
Initial	Residual*	Front	Back	Front	Back	Front	Back	Initial	Residual
Steel Target Plate									
1700	---	12,500	7,800	14.0	8.0	2700	>2800	20.2	---
2000	400	6,200	5,400	7.4	8.6	2700	2400	16.9	9.6
2300	---	19,900	6,100	24.5	6.5	2600	>2800	21.1	17.0
2600	---	4,500	3,000	7.0	4.5	2600	2500	20.1	15.9
3100	900	6,900	11,600	9.0	16.0	2700	2300	17.0	7.4
4200	1400	5,000	6,000	5.2	7.0	2700	>2800	14.9	1.0
Titanium Target Plate									
1800	900	7,100	4,300	8.5	6.5	2600	2300	17.7	11.0
3000	1000	6,300	7,300	10.0	12.0	2600	2300	16.6	10.9
4000	1500	7,700	21,200	9.0	33.0	2600	2400	17.6	1.8
Aluminum Target Plate									
2300	---	2,700	1,600	4.0	2.5	2600	2600	17.5	13.0
2500	1000	1,700	1,200	2.5	2.0	2500	2600	18.6	15.9
2900	1100	2,000	1,100	3.5	2.0	2600	>2800	17.4	8.0
3100	1300	2,800	8,900	4.0	12.0	2600	>2800	17.6	4.7
3600	1700	2,800	17,000	4.0	20.0	2600	2800	18.3	3.0
3700	---	4,000	37,800	5.0	42.0	2600	>2800	17.5	4.7

*Determined from flash X-ray.

--- Data not obtained

TABLE VII. TERMINAL EFFECTS ALLOY 29 (MRE + 4% ALUMINUM)

Velocity (fps)		Thermal Energy (watt-sec/m^2)		Event Duration (milliseconds)		Peak Temperature (°C)		Mass (grains)	
Initial	Residual*	Front	Back	Front	Back	Front	Back	Initial	Residual
Steel Target Plate									
1400	---	6,900	**	9.0	**	2600	**	19.6	**
1600	---	6,900	**	9.0	**	2600	**	19.4	**
2300	---	7,800	3,800	10.5	6.0	2600	2500	19.7	16.3
2800	---	5,400	3,600	8.0	6.0	2600	2500	19.6	15.7
3000	---	38,700	39,100	45.5	45.5	2600	2500	19.9	7.8
3100	800	---	---	---	---	---	---	19.6	3.5
3100	---	23,800	31,300	36.0	40.5	2600	2700	19.5	7.7
Titanium Target Plate									
1900	600	11,300	4,300	14.0	6.8	2400	2700	19.9	16.9
3100	1200	6,300	2,600	7.5	2.5	2700	>2800	20.2	14.8
4200	1800	13,200	18,900	17.0	24.0	2600	>2800	19.6	2.3
Aluminum Target Plate									
2000	900	2,100	2,400	3.2	3.8	2600	2300	19.3	18.4
4100	1900	4,300	34,100	7.0	46.0	2600	2600	19.5	1.7

* Determined from flash X-ray.

** Projectile did not penetrate target.

--- Data not obtained.

TABLE VIII. TERMINAL EFFECTS (ZIRCONIUM)

Steel Target Plate

Velocity (fps)		Thermal Energy (watt-sec/in^2)		Event Duration (milliseconds)		Peak Temperature (°C)		Mass (grains)	
Initial	Residual*	Front	Back	Front	Back	Front	Back	Initial	Residual
2000	600	300	200	0.6	0.2	2500	2100	19.7	19.6
2100	---	2,100	800	3.0	1.5	2600	2400	20.4	18.9
2200	---	3,200	3,000	5.0	5.0	2500	2300	20.1	19.1
2200	---	2,500	3,300	5.0	5.5	2600	2500	20.4	19.2
2300	---	1,400	700	2.5	1.5	2300	2400	20.5	19.2
2400	---	7,200	2,800	12.0	4.0	2500	2500	20.1	18.9
2400	---	1.800	600	3.0	1.0	2500	2400	20.3	18.9
2500	---	3,300	1,700	6.0	3.5	2500	2400	20.3	18.8
2900	1000	3,600	2,500	3.5	4.5	2800	2100	19.7	19.1
3800	---	16,600	16,500	21.0	21.0	2500	2500	19.9	15.8
4100	1600	15,400	16,000	11.0	12.0	2600	2500	19.8	17.2
4500	---	16,400	17,300	20.0	20.0	2600	2600	19.6	12.9
4800	---	11,100	20,600	14.0	24.5	2700	2800	20.4	15.9
5000	---	34,100	39,600	41.0	45.0	2600	2600	20.7	14.8

* Determined from flash X ray.

--- Data not obtained.

TABLE VIII. TERMINAL EFFECTS (ZIRCONIUM) (CONCLUDED)

Aluminum Target Plate

Velocity (fps)		Thermal Energy (watt-sec/m^2)		Event Duration (milliseconds)		Peak Temperature (^oC)		Mass (grains)	
Initial	Residual*	Front	Back	Front	Back	Front	Back	Initial	Residual
2900	1400	1,000	900	1.5	1.5	2600	2500	20.1	---
3400	1400	300	700	1.0	1.5	2400	2400	19.9	19.4
4000	1700	1,000	900	2.0	1.5	2600	2500	20.5	19.5
4500	1800	2,100	18,400	4.0	24.5	2600	2500	19.8	16.8
5000	1800	3,500	17,000	5.5	20.5	2600	2500	20.1	10.9

Titanium Target Plate

2000	700	1,300	900	2.2	1.6	2500	2100	19.5	19.4
2900	1100	6,800	2,400	10.5	4.5	2600	2200	20.0	19.8
4000	1700	3,200	11,100	5.0	19.0	2600	2200	20.0	16.6

* Determined from flash X-ray

--- Data not obtained.

TABLE IX. TERMINAL EFFECTS (ZIRCONIUM-TIN)

Velocity (fps)		Thermal Energy (watt-sec/m^2)		Event Duration (milliseconds)		Peak Temperature (°C)		Mass (grains)	
Initial	Residual*	Front	Back	Front	Back	Front	Back	Initial	Residual
Steel Target Plate									
2000	600	1,100	200	1.2	0.4	2600	1900	19.8	19.7
2900	1000	2,500	1,500	1.8	2.4	2800	2100	19.9	19.3
3000	---	4,200	4,100	6.5	7.0	2600	2500	21.5	18.8
3000	---	2,000	2,800	3.0	4.0	2500	2500	21.9	18.9
3500	---	12,200	20,900	17.0	26.0	2600	>2800	21.0	19.1
3600	---	6,800	5,500	8.0	7.0	2600	2600	20.4	---
4000	1500	2,500	5,100	3	7.0	2500	2400	19.8	16.9
4000	---	3,700	4,200	5.5	5.5	2500	2600	20.0	18.3
4700	---	23,200	37,900	27.0	44.5	2600	2600	20.2	13.1
5000	---	24,600	41,400	28.0	45.5	2600	2700	20.2	11.4
Titanium Target Plate									
2000	700	1,400	4,000	2.4	8.4	2500	2000	19.3	19.2
2800	900	1,300	900	1.8	1.4	2500	2100	19.8	19.6
4200	1700	4,000	12,900	6.2	17.2	2700	2500	19.7	17.5

* Determined from flash X-ray.

--- Data not obtained.

TABLE IX. TERMINAL EFFECTS (ZIRCONIUM-TIN) (CONCLUDED)

Aluminum Target Plate

Velocity (fps)		Thermal Energy (watt-sec/m^2)		Event Duration (milliseconds)		Peak Temperature (^oC)		Mass (grains)	
Initial	Residual*	Front	Back	Front	Back	Front	Back	Initial	Residual
3000	1300	700	1,000	1.5	2.0	2600	2500	19.8	19.1
3500	1500	700	700	1.5	1.5	2500	2500	20.6	20.4
4000	1800	900	14,700	2.0	20.0	2500	2400	20.3	18.6
4000	1800	11,300	31,700	21.0	39.5	2600	2600	19.4	17.4
5000	1900	1,900	5,400	3.5	7.5	2600	2600	20.0	18.5

* Determined from flash X-ray

TABLE X. DEPLETED URANIUM

Steel Target Plate

Velocity (fps)		Thermal Energy (watt-sec/m^2)		Event Duration (milliseconds)		Peak Temperature (°C)		Mass (grains)	
Initial	Residual*	Front	Back	Front	Back	Front	Back	Initial	Residual
1400	500	700	200	10.2	0.4	2400	1900	23.2	23.2
3000	1300	1,400	7,000	2.0	11.8	2600	2400	22.1	20.0
4900	2100	4,500	11,400	3.5	3.0	2600	2600	22.4	10.4
				Titanium Target Plate					
1500	500	600	1,000	0.8	14	2300	2400	22.9	22.9
2900	1300	1,500	600	1.8	0.8	2600	2400	22.3	22.3
4800	2300	5,200	14,300	8.2	18.2	2500	2500	21.6	6.2
				Aluminum Target Plate					
1500	700	800	**	1.6	0	2400	0	22.8	22.8
2900	1500	1,100	100	1.2	0.2	2700	1900	21.8	21.8
4700	2100	1,600	5,100	2.0	8.4	2600	2400	22.9	15.2

* Determined from flash X-ray.

** Projectile did not penetrate target.

TABLE XI. ALLOY 14 (MRE + 10% BISMUTH)

Aluminum Target Plate

Test Data

Velocity (fps)		Thermal Energy (watt-sec/m^2)	
Initial	Residual	Front	Back
2550	880	3,200	1,700
2600	1150	2,800	1,100
2720	-	1,800	1,800
2960	1300	2,500	1,800
3030	1330	1,700	14,400
3470	1530	2,000	2,600
3610	1510	4,500	26,900
3980	-	3,000	23,500
4180	-	2,100	43,100
5010	-	3,100	46,500
5050	-	3,600	87,800
	Smoothed Data		
1000	-	1,900	100
2000	-	2,200	700
3000	-	2,500	3,600
4000	-	2,800	17,800
5000	-	3,100	88,300
6000	-	3,600	436,900
	Titanium Target Plate		
	Test Data		
1990	880	20,100	14,400
2760	-	7,400	4,000
2910	1060	8,600	6,000
4010	-	3,800	44,100
4040	1550	13,600	37,200
4910	-	4,000	77,400
5030	-	1,900	52,500

- Data not obtained.

TABLE XI. ALLOY 14 (MRE + 10% BISMUTH) (CONCLUDED)

Titanium Target Plate

Smoothed Data

Velocity (fps)		Thermal Energy (watt-sec/m^2)	
Initial	Residual	Front	Back
1000	-	29,100	2,500
2000	-	16,600	5,600
3000	-	9,500	72,600
4000	-	5,400	28,600
5000	-	3,100	64,700
6000	-	1,800	146,500

Steel Target Plate

Test Data

1580	-	5,200	*
1700	-	7,800	*
2060	650	5,500	6,100
2580		6,700	3,200
2640	-	4,900	2,300
2950	1050	3,800	8,800
4200	1643	7,800	12,000

Smoothed Data

1000	-	5,400	2,000
2000	-	5,700	3,400
3000	-	5,900	5,800
4000	-	6,100	9,800
5000	-	6,400	16,500
6000	-	6,600	27,900

- Data not obtained

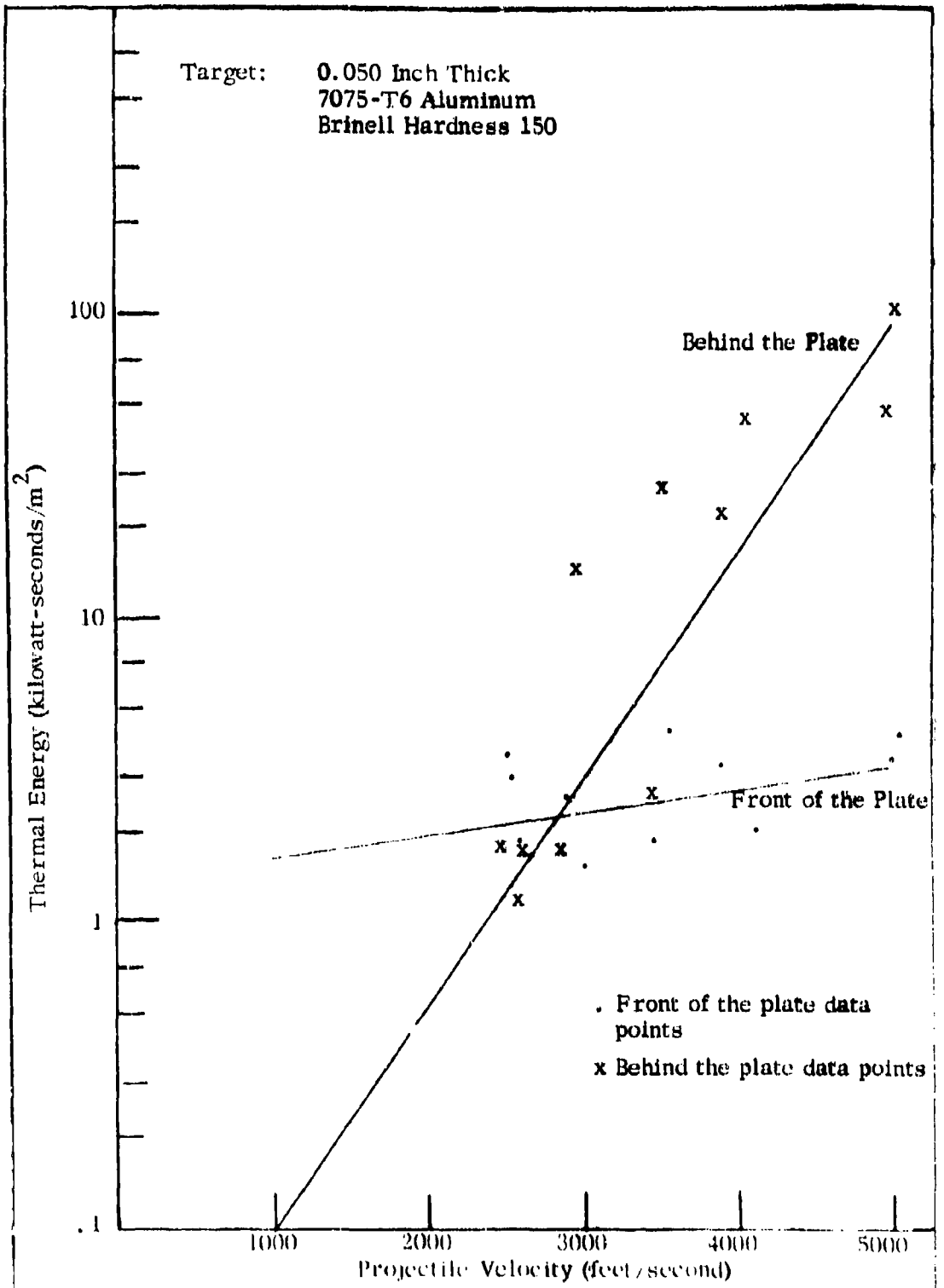

Figure 15. Thermal Energy Versus Projectile Velocity for MRE + 10 % Bismuth against Aluminum Target Plate

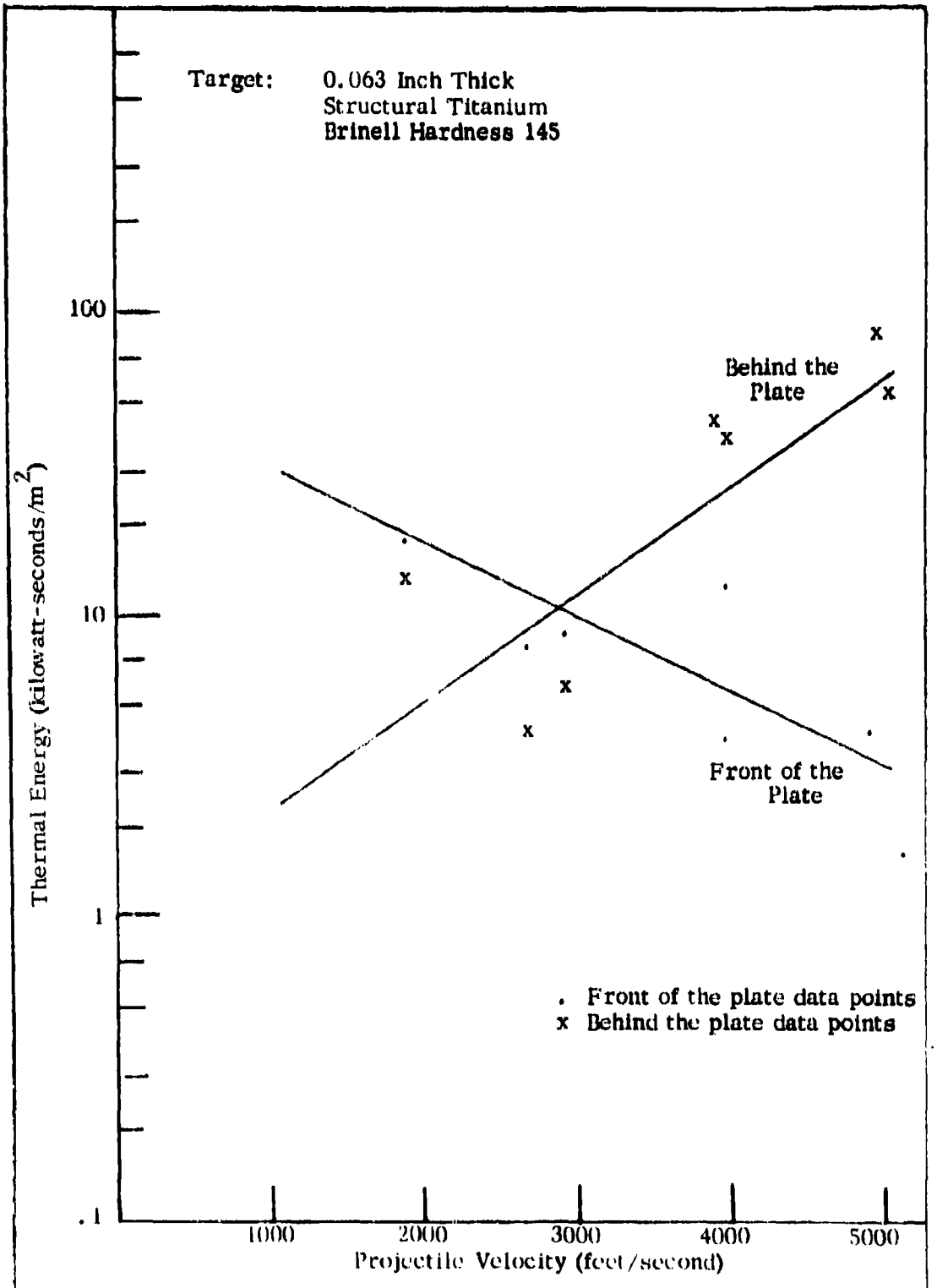

Figure 16. Thermal Energy Versus Projectile Velocity for MRE + 10 % Bismuth against Titanium Target Plate

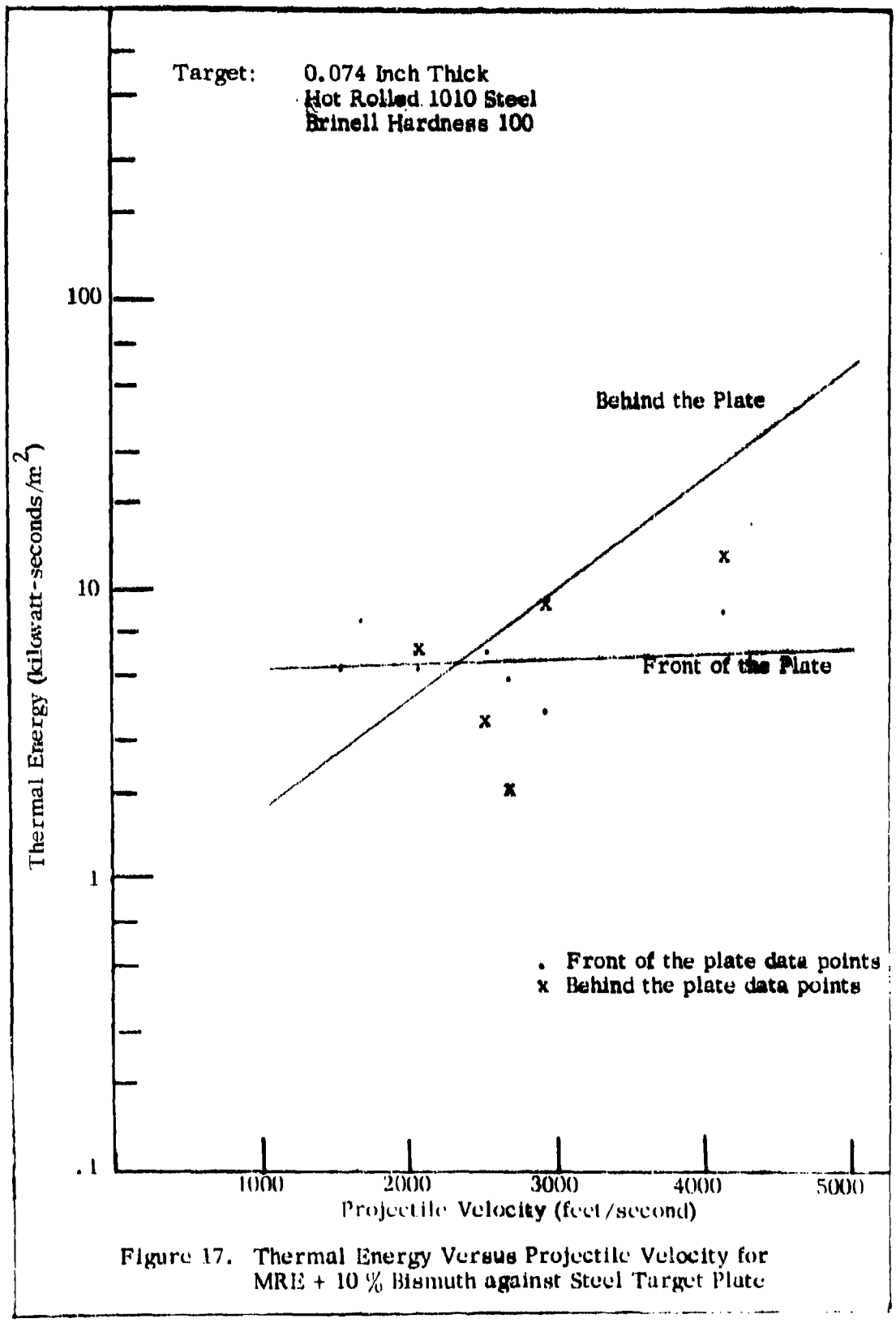

Figure 17. Thermal Energy Versus Projectile Velocity for MRE + 10 % Bismuth against Steel Target Plate

TABLE XII. ALLOY 19 (MRE +5% MAGNESIUM)

Aluminum Target Plate

Test Data

Velocity (fps)		Thermal Energy (watt-sec/m²)	
Initial	Residual	Front	Back
2330	-	6,300	5,500
2530	1025	12,500	7,800
2910	1177	19,900	6,100
3060	1295	4,500	3,000
3620	1668	6,900	11,600
3740	-	5,000	6,000
	Smoothed Data		
1000	-	17,000	4,200
2000	-	11,600	5,100
3000	-	8,000	6,100
4000	-	5,500	7,400
5000	-	3,700	8,800
6000	-	2,600	10,600

Titanium Target Plate

Test Data

1820	880	7,100	4,400
2970	1030	6,300	7,300
4040	1550	7,700	21,300
	Smoothed Data		
1000	-	6,600	2,200
2000	-	6,800	4,500
3000	-	7,000	9,200
4000	-	7,300	18,600
5000	-	7,500	37,700
6000	-	7,800	76,500

- Data not obtained

TABLE XII. ALLOY 19 (MRE +5% MAGNESIUM) (CONCLUDED)

Steel Target Plate

Test Data

Velocity (fps)		Thermal Energy (watt-sec/in^2)	
Initial	Residual	Front	Back
1720	-	6,700	5,000
2040	430	6,300	1,400
2060	-	6,400	1,830
2290	-	7,000	600
2550	-	5,500	3,100
2700	-	6,100	1,000
3090	920	6,500	7,800
4240	1380	7,000	5,500
	Smoothed Data		
1000	-	6,200	1,130
2000	-	6,300	1,800
3000	-	6,500	3,000
4000	-	6,600	4,600
5000	-	6,800	7,400
6000	-	7,000	11,800

- Data not obtained.

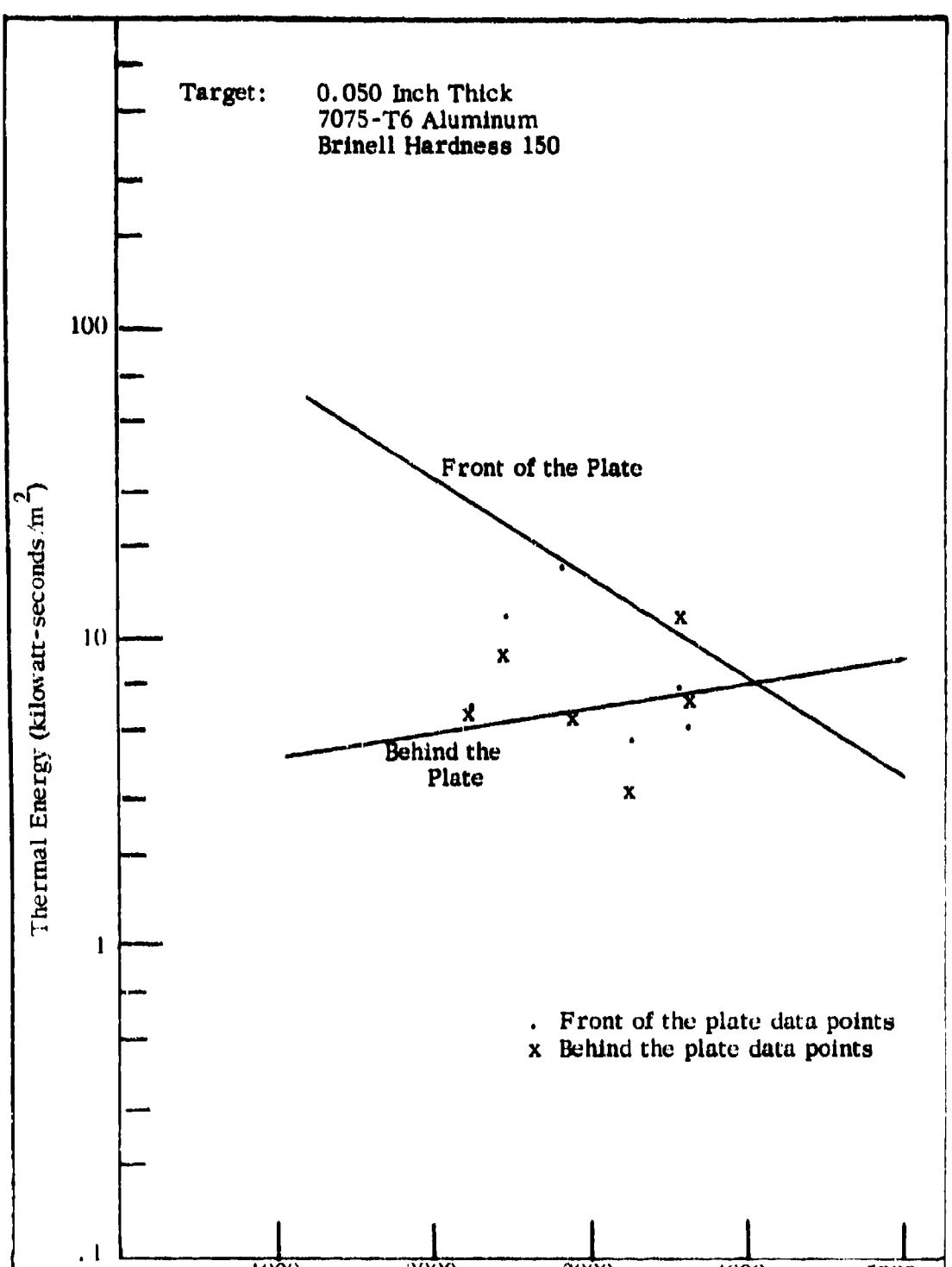

Figure 18. Thermal Energy Versus Projectile Velocity for MRE + 5% Magnesium against Aluminum Target Plate

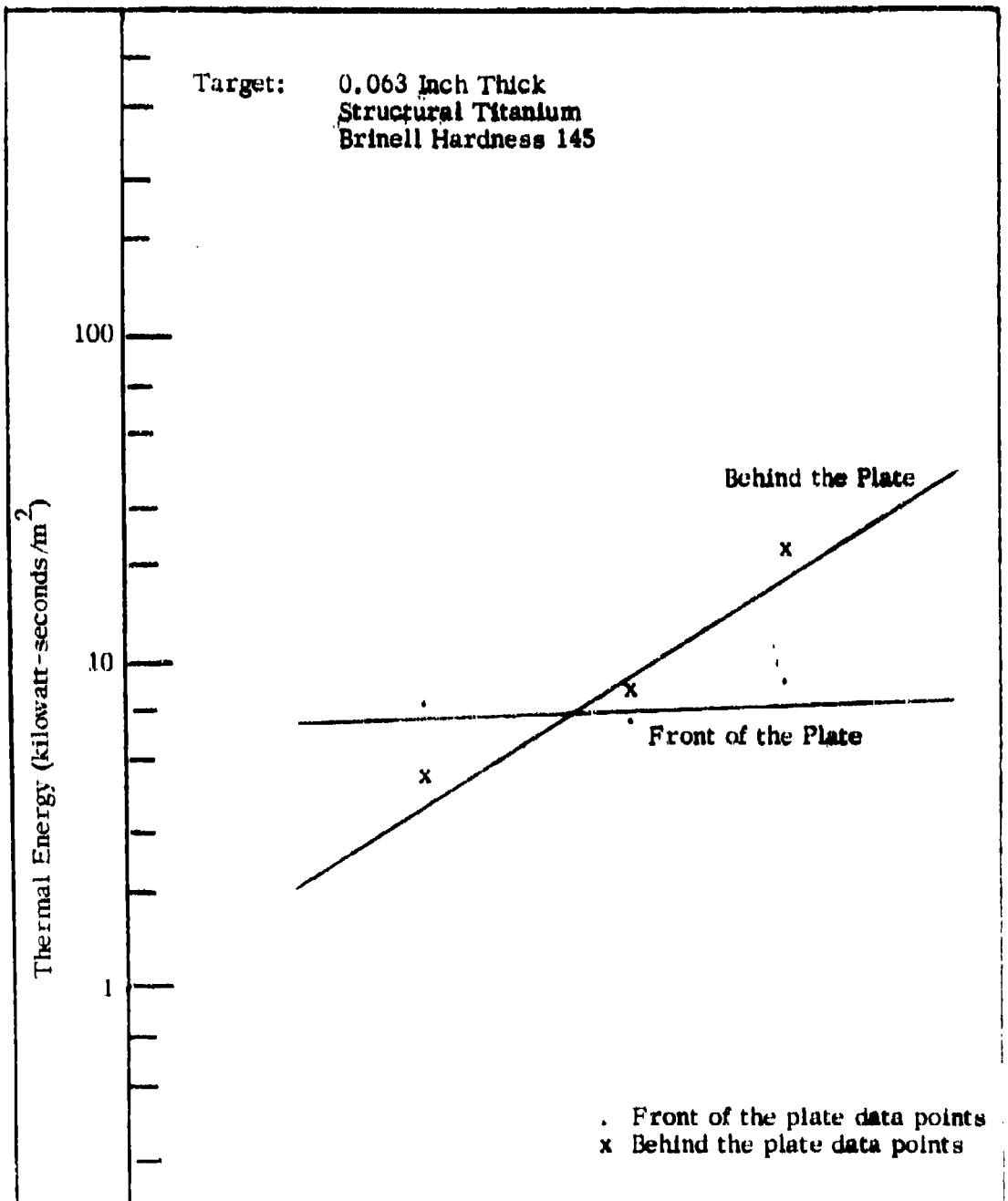

Figure 19. Thermal Energy Versus Projectile Velocity for MRE + 5 % Magnesium against Titanium Target Plate

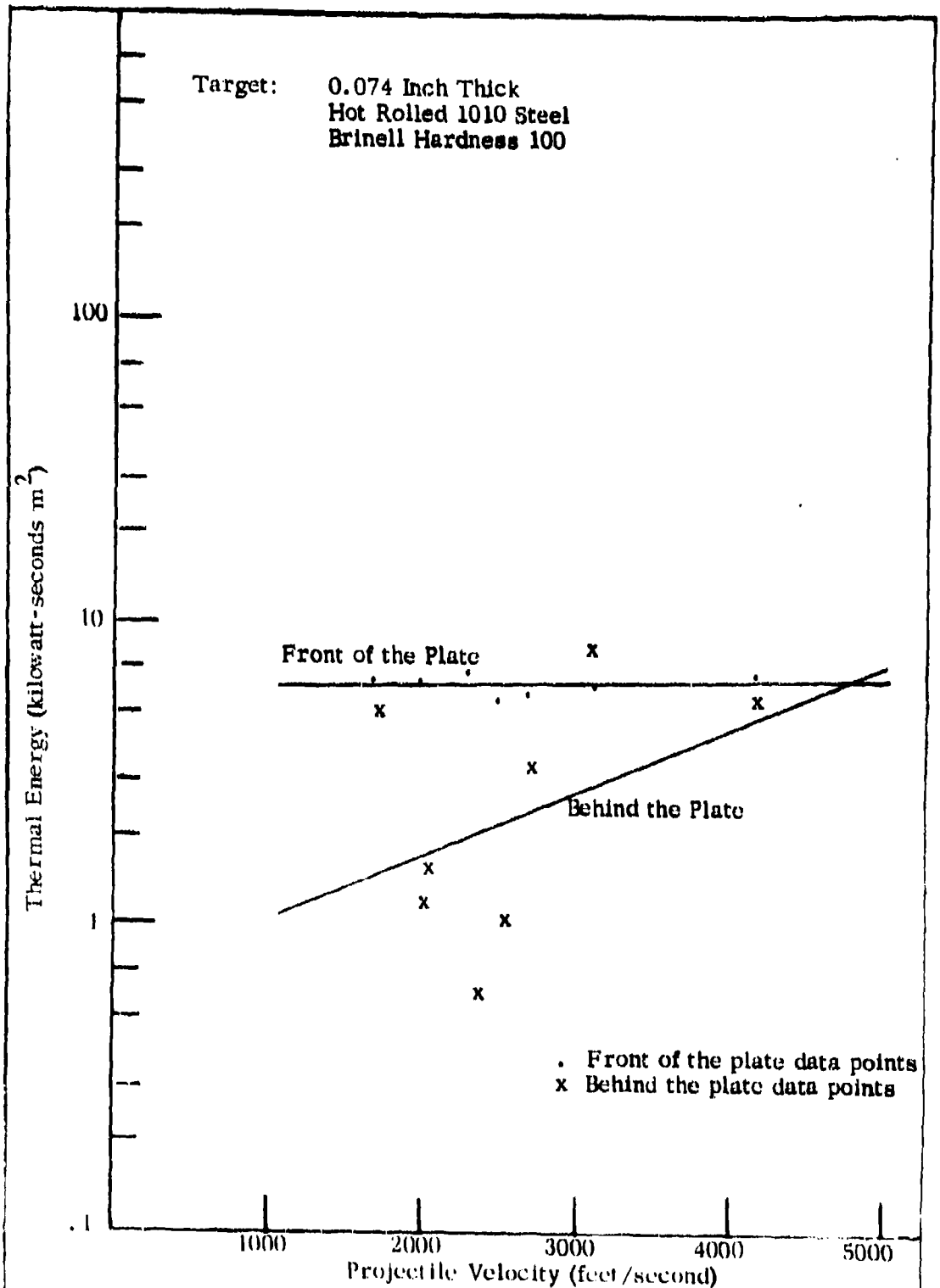

Figure 20. Thermal Energy Versus Projectile Velocity for MRE + 5 % Magnesium against Steel Target Plate

TABLE XIII. ALLOY 29 (MRE + 4% ALUMINUM)

Aluminum Target Plate

Test Data

Velocity (fps)		Thermal Energy (watt-sec/m^2)	
Initial	Residual	Front	Back
2030	900	2,100	2,400
4110	1900	4,300	34,100
	Smoothed Data		
1000	-	1,500	600
2000	-	2,100	2,300
3000	-	2,900	8,300
4000	-	4,100	29,600
5000	-	5,800	106,100
6000	-	8,300	380,200
	Titanium Target Plate		
	Test Data		
1920	650	11,300	4,300
3130	1160	6,300	2,600
4250	1810	13,200	19,000
	Smoothed Data		
1000	-	8,600	1,600
2000	-	9,200	3,000
3000	-	9,700	5,600
4000	-	10,300	10,500
5000	-	11,000	19,500
6000	-	11,600	36,400

- Data not obtained.

TABLE XIII. ALLOY 29 (MRE + 4% ALUMINUM) (CONCLUDED)

Steel Target Plate

Test Data

Velocity (fps)		Thermal Energy (watt-sec/m^2)	
Initial	Residual	Front	Back
1450	-	6,900	*
1600	-	7,000	*
2270	-	7,800	4,000
2760	-	5,400	3,600
3050	-	38,700	39,100
3090	819	-	-
3120	-	23,800	31,300
	Smoothed Data		
1000	-	4,000	100
2000	-	8,400	1,300
3000	-	17,700	20,000
4000	-	37,500	314,000
5000	-	79,400	4.9×10^6
6000	-	160,000	7.8×10^7

*Did not penetrate.

- Data not obtained.

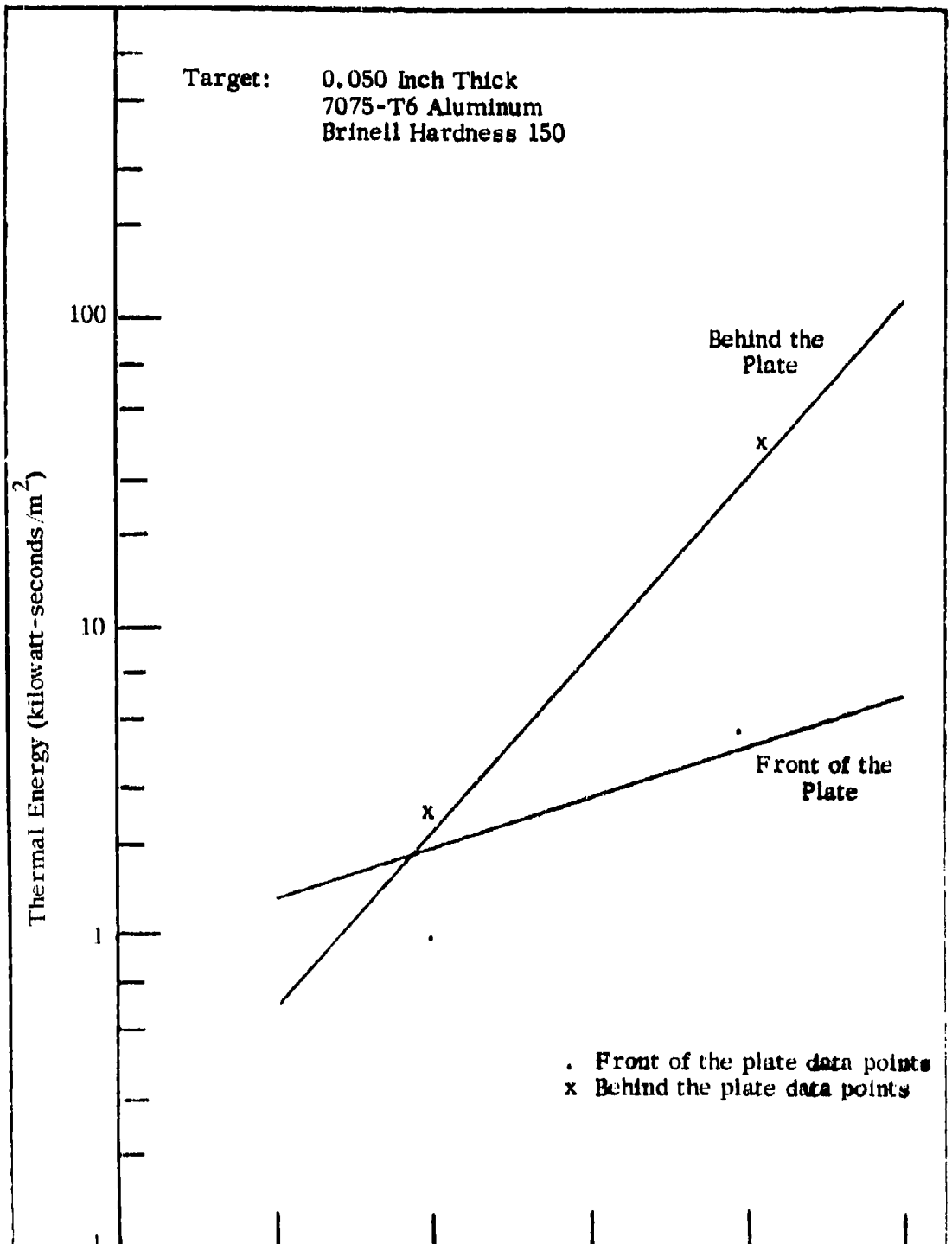

Figure 21. Thermal Energy Versus Projectile Velocity for MRE + 4 % Aluminum against Aluminum Target Plate

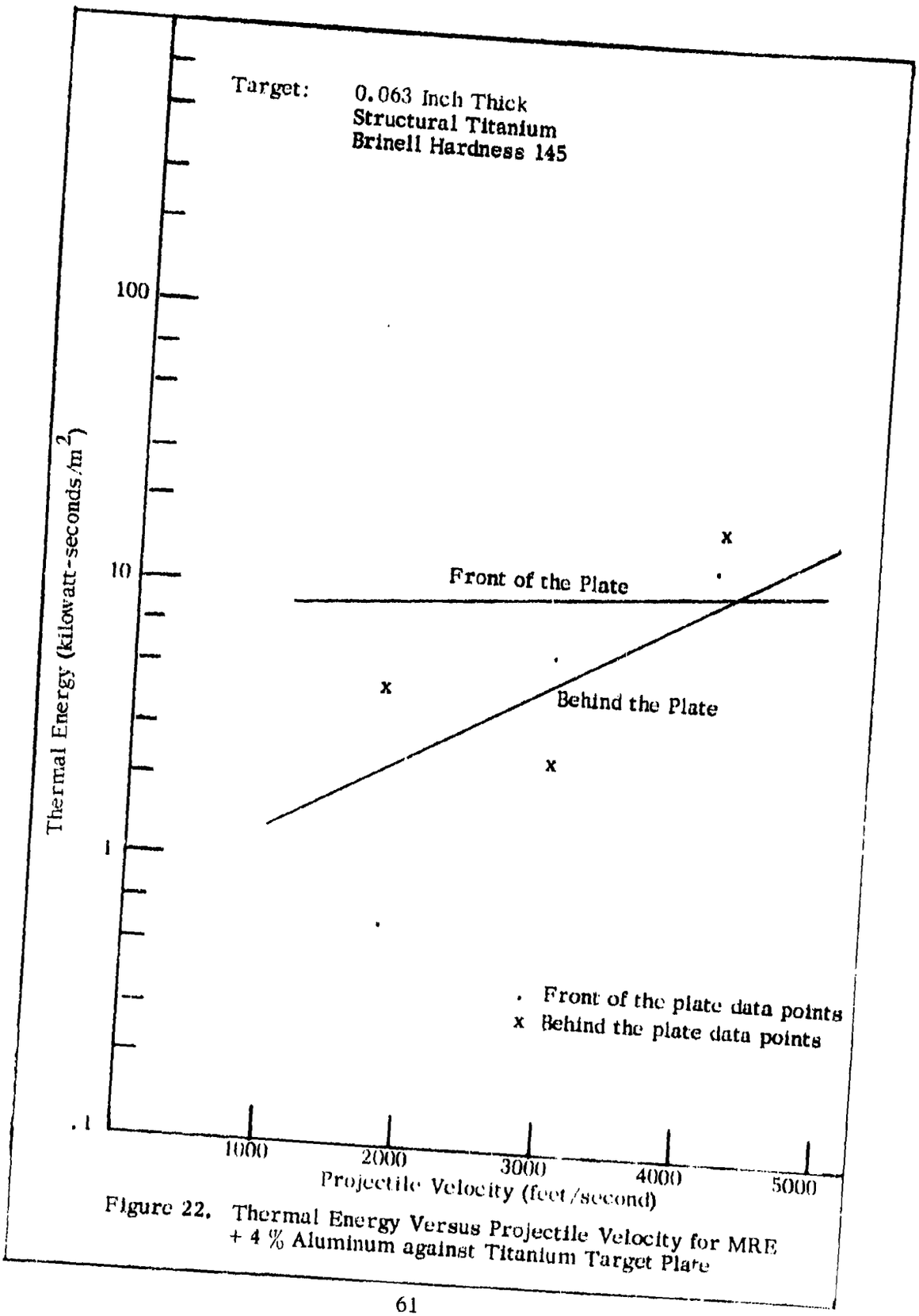

Figure 22. Thermal Energy Versus Projectile Velocity for MRE + 4 % Aluminum against Titanium Target Plate

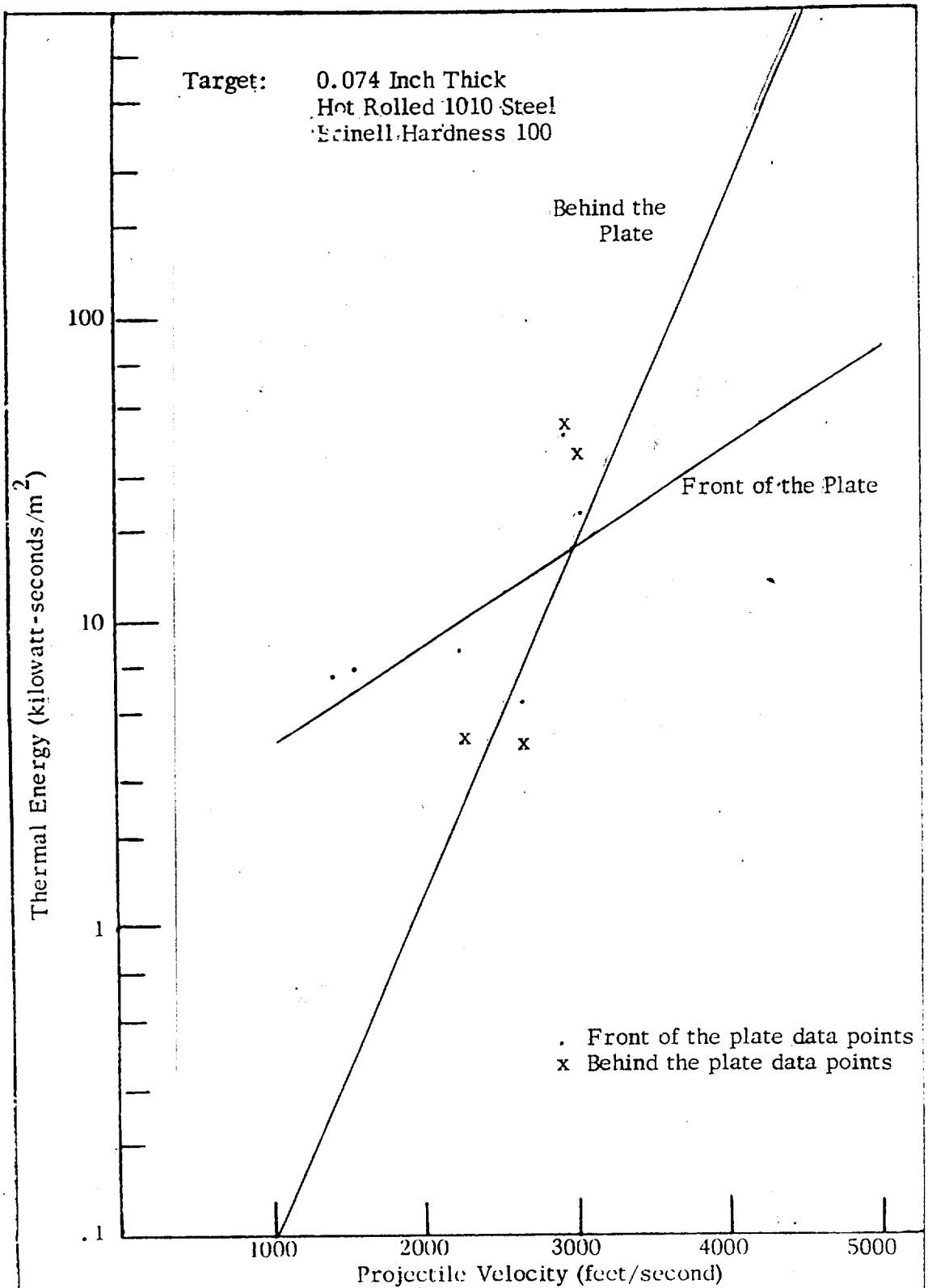

Figure 23. Thermal Energy Versus Projectile Velocity for MRE + 4 % Aluminum against Steel Target Plate

TABLE XIV. ZIRCONIUM

Aluminum Target Plate

Test Data

Velocity (fps)		Thermal Energy (watt-sec/m^2)	
Initial	Residual	Front	Back
2900	1400	1,000	900
3400	1500	300	700
4100	1700	1,000	900
4500	1800	2,100	18,400
5000	1800	3,500	17,000

Smoothed Data

1000	-	100	0
2000	-	200	100
3000	-	500	500
4000	-	1,200	2,900
5000	-	2,800	16,400
6000	-	6,400	91,000

Titanium Target Plate

Test Data

2000	700	1,300	900
2900	1100	6,800	2,400
4100	1700	3,200	11,100

Smoothed Data

1000	-	1,400	300
2000	-	2,100	900
3000	-	3,100	3,000
4000	-	4,600	10,000
5000	-	6,800	33,300
6000	-	10,100	111,200

- Data not obtained.

TABLE XIV. ZIRCONIUM (CONCLUDED)

Steel Target Plate

Test Data

Velocity (fps)		Thermal Energy (watt-sec/m^2)	
Initial	Residual	Front	Back
2000	600	300	200
2100	-	2,100	800
2200	-	3,200	3,000
2200	-	2,500	3,300
2300	-	1,400	700
2400	-	7,200	2,800
2500	-	1,800	600
2500	-	3,300	1,700
2900	1000	3,000	2,000
3900	-	16,600	16,500
4100	1600	15,400	16,000
4500	-	16,400	17,300
4800	-	11,100	20,600
5000	-	34,100	39,600
	Smoothed Data		
1000	-	600	200
2000	-	1,600	800
3000	-	4,200	3,000
4000	-	11,100	10,900
5000	-	29,200	39,400
6000	-	77,300	143,000

- Data not obtained.

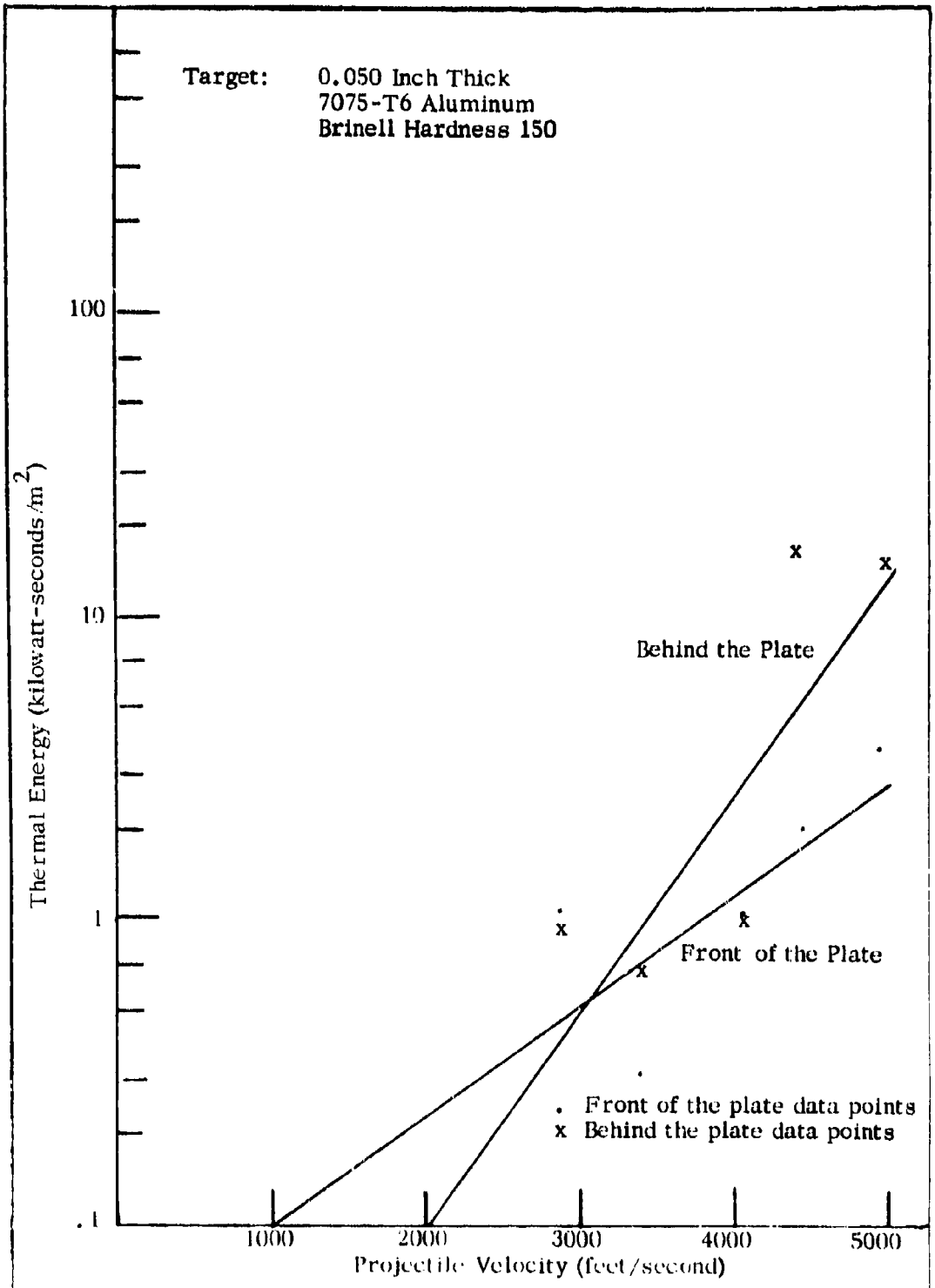

Figure 24. Thermal Energy Versus Projectile Velocity for Zirconium against Aluminum Target Plate

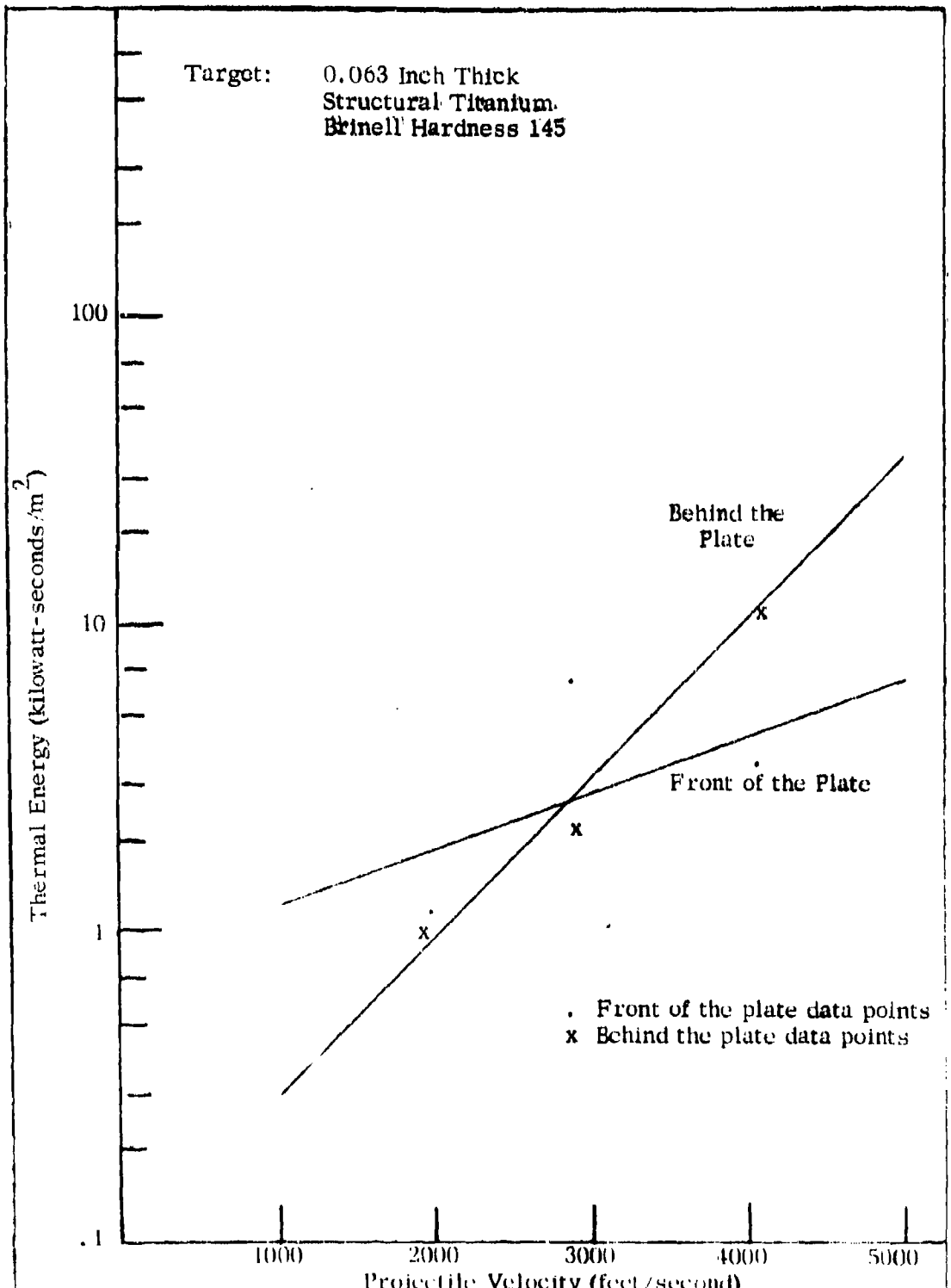

Figure 25. Thermal Energy Versus Projectile Velocity for Zirconium against Titanium Target Plate

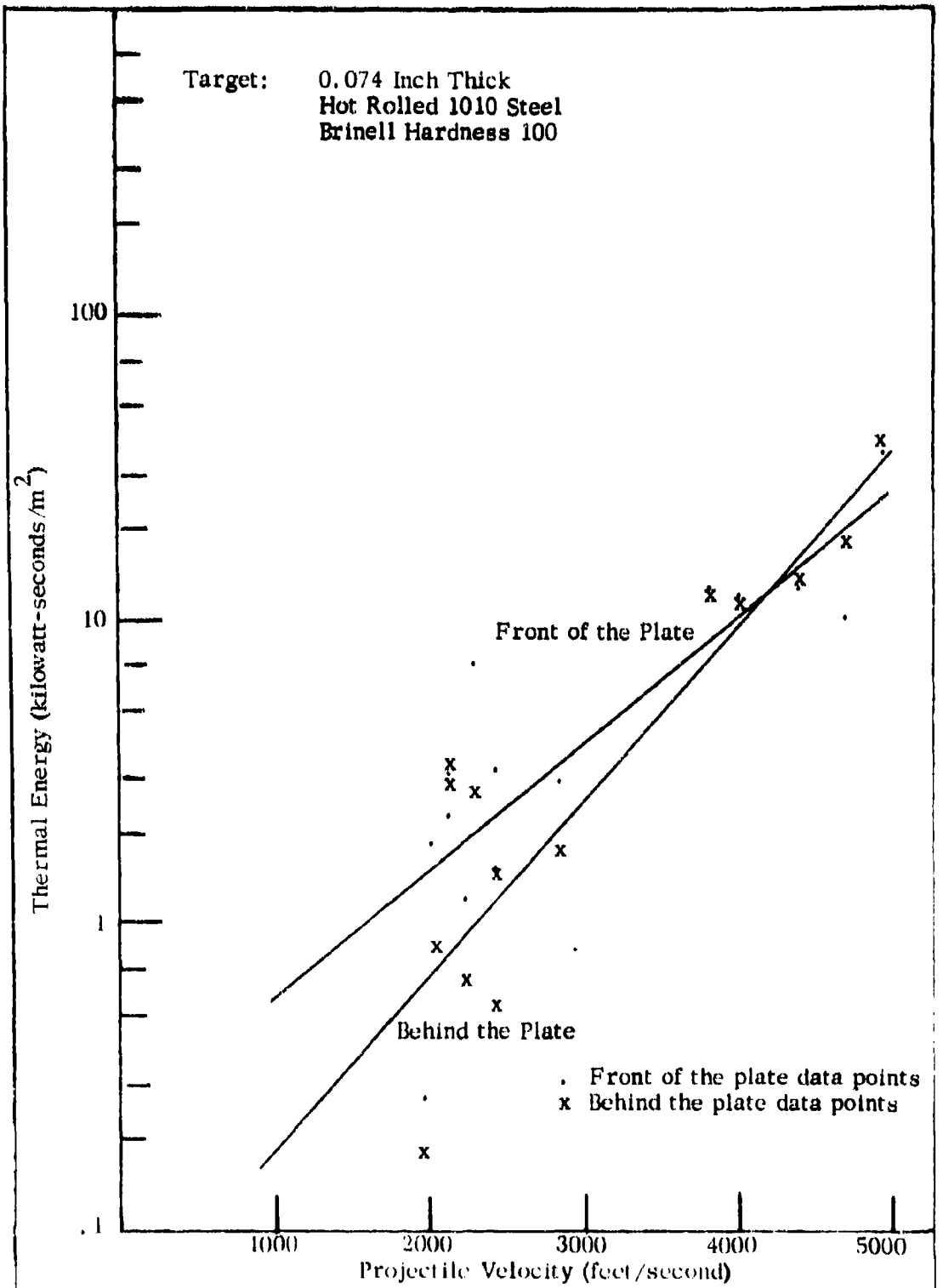

Figure 26. Thermal Energy Versus Projectile Velocity for Zirconium against Steel Target Plate

TABLE XV. ZIRCONIUM-TIN

Aluminum Target Plate

Test Data

Velocity (fps)		Thermal Energy (watt-sec/m^2)	
Initial	Residual	Front	Back
3000	1300	700	1,000
3500	1500	700	700
4000	1800	900	14,700
4600	1800	11,300	31,700
5000	2000	1,900	5,400
	Smoothed Data		
1000	-	100	100
2000	-	200	200
3000	-	600	1,000
4000	-	1,600	4,500
5000	-	4,300	19,400
6000	-	11,600	84,200
	Titanium Target Plate		
	Test Data		
2000	700	1,400	400
2800	900	1,300	900
4200	1700	4,000	12,900
	Smoothed Data		
1000	-	700	100
2000	-	1,200	300
3000	-	1,900	1,700
4000	-	3,200	8,500
5000	-	5,400	43,000
6000	-	9,000	214,400

- Data not obtained.

TABLE XV. ZIRCONIUM-TIN (CONCLUDED)

Steel Target Plate

Test Data

Velocity (fps)		Thermal Energy (watt-sec/m^2)	
Initial	Residual	Front	Back
2000	600	1,000	200
3000	1000	2,500	1,500
3000	-	4,200	4,100
3000	-	2,000	2,800
3500	-	12,200	20,900
3600	-	6,800	5,500
4000	1500	2,500	5,100
4000	-	3,700	4,200
4700	-	23,200	37,900
5000	-	24,600	41,400
	Smoothed Data		
1000	-	400	100
2000	-	1,100	400
3000	-	2,900	2,100
4000	-	7,500	10,100
5000	-	19,800	48,200
6000	-	52,000	229,800

- Data not obtained.

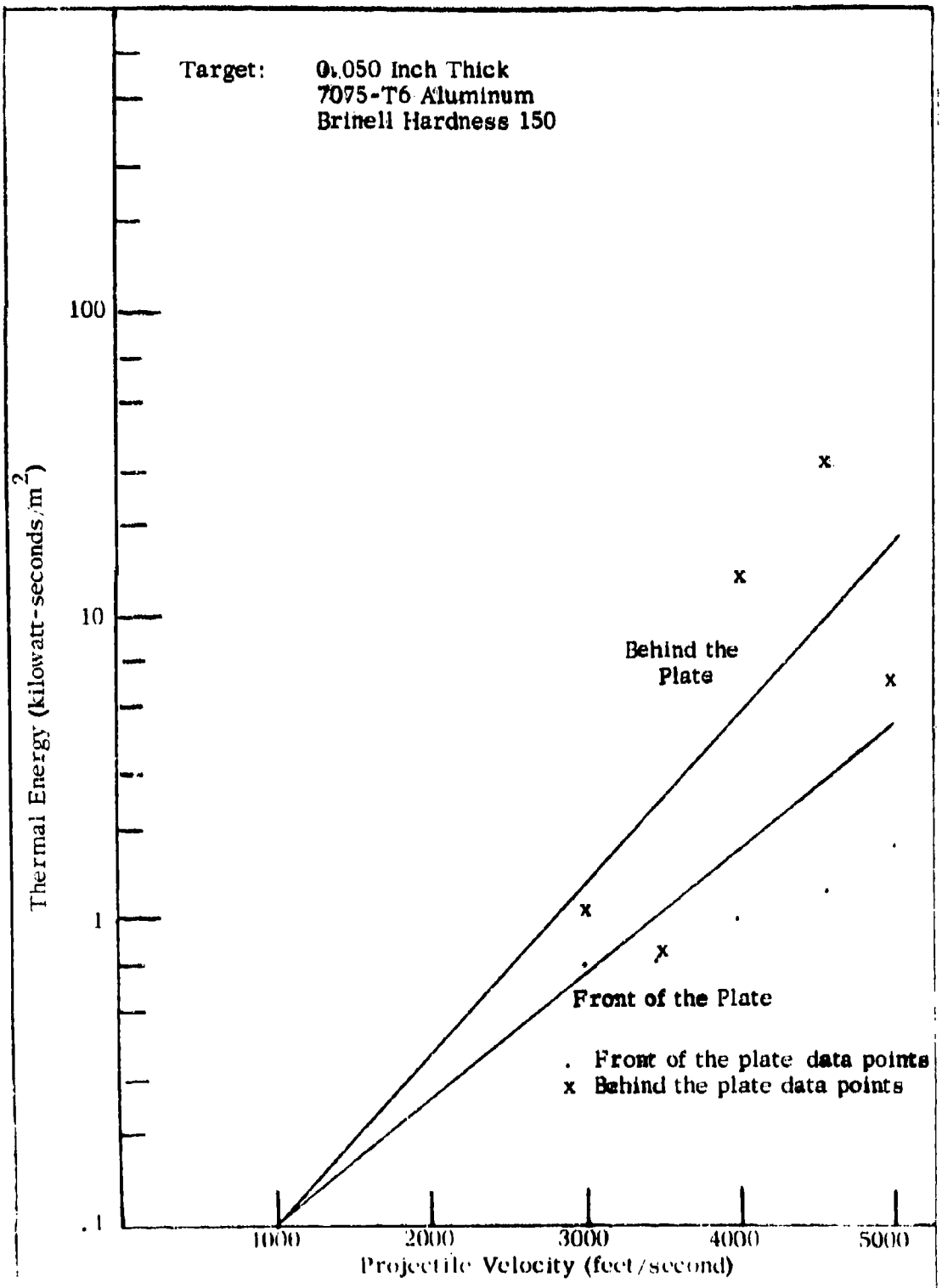

Figure 27. Thermal Energy Versus Projectile Velocity for Zirconium-Tin against Aluminum Target Plate

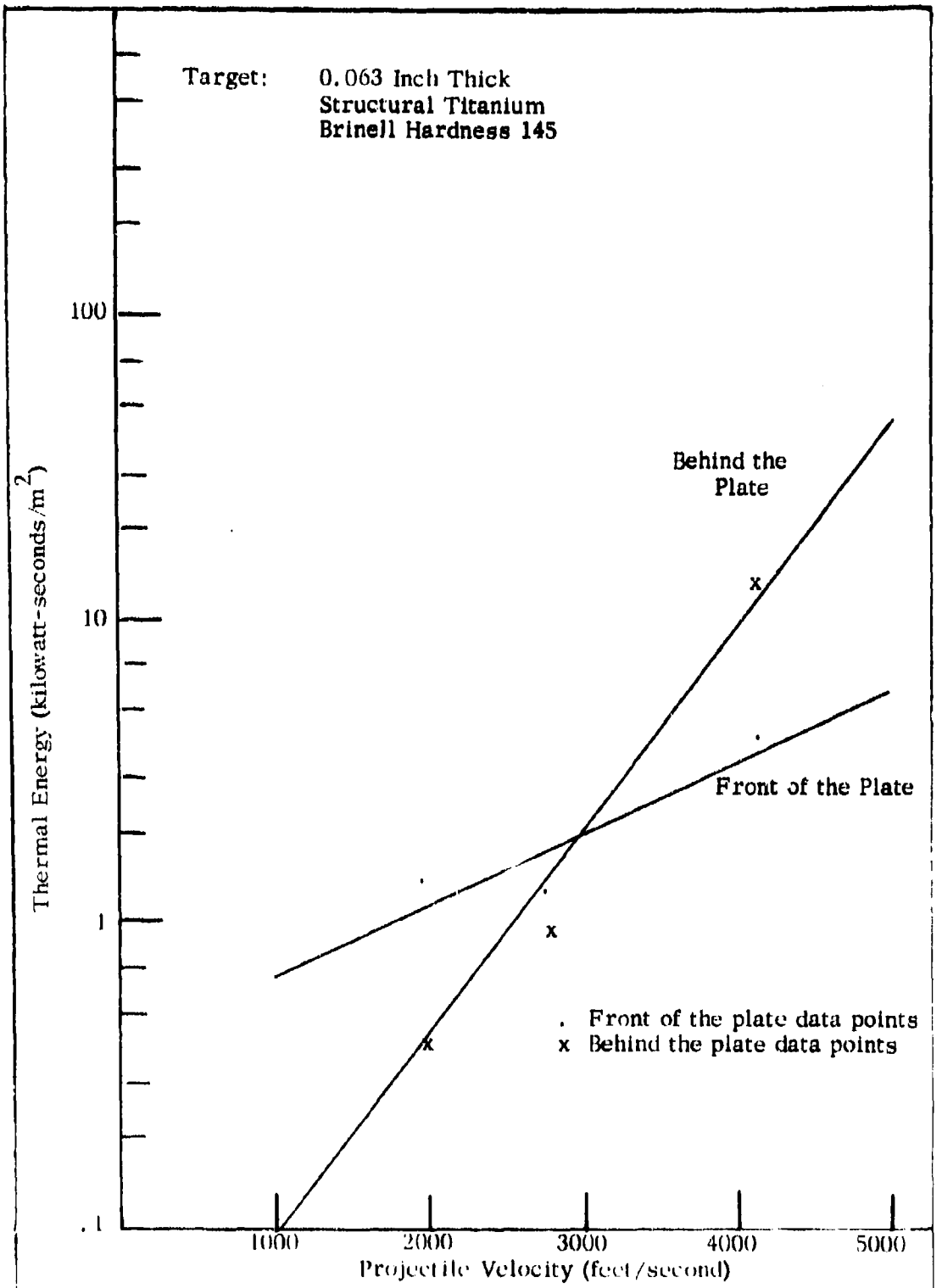

Figure 28. Thermal Energy Versus Projectile Velocity for Zirconium-Tin against Titanium Target Plate

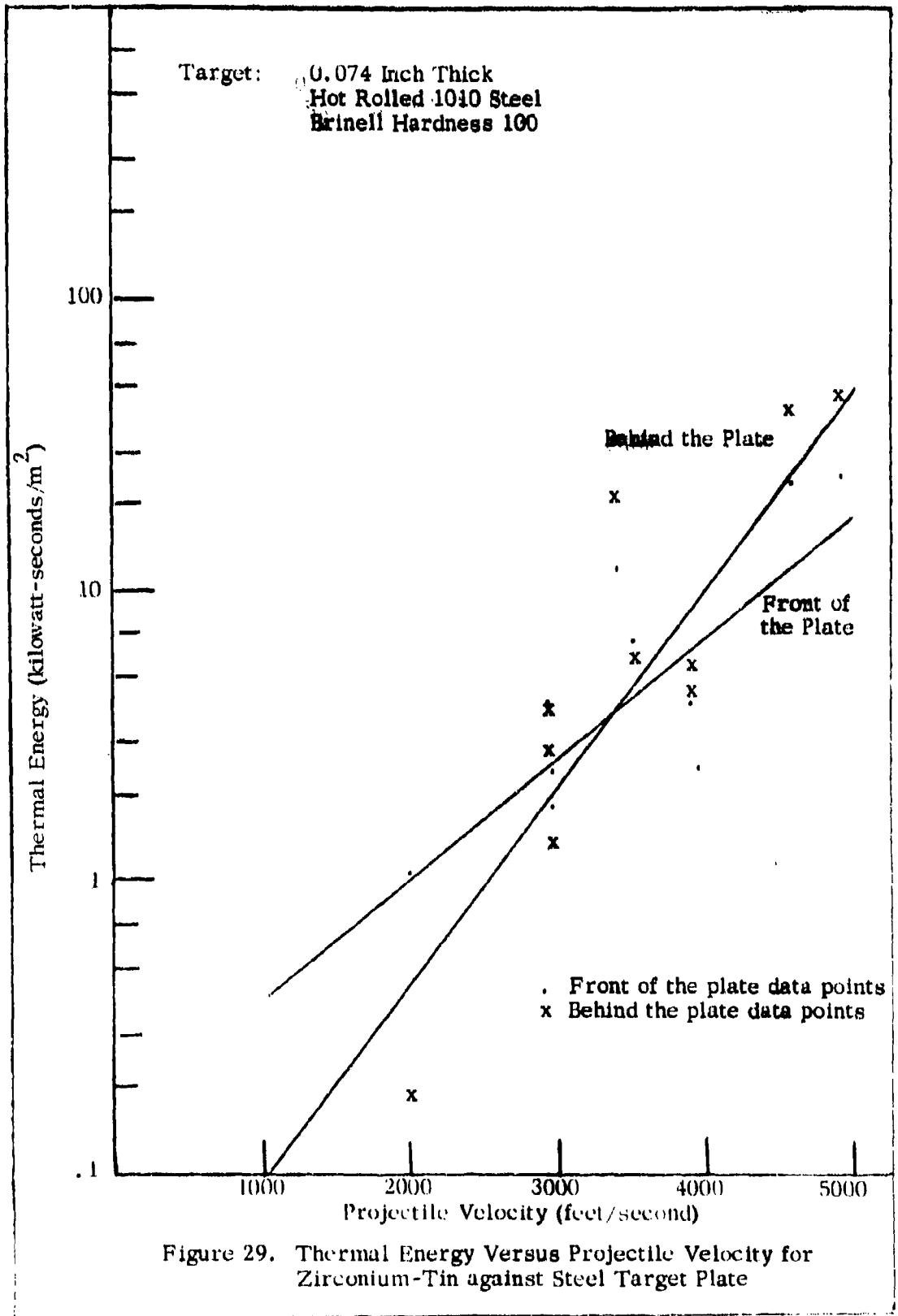

Figure 29. Thermal Energy Versus Projectile Velocity for Zirconium-Tin against Steel Target Plate

TABLE XVI. DEPLETED URANIUM

Aluminum Target Plate

Test Data

Velocity (fps)		Thermal Energy (watt-sec/m^2)	
Initial	Residual	Front	Back
1500	700	800	0
2900	1600	1,100	100
4700	2100	1,600	5,100
	Smoothed Data		
1000	-	700	0
2000	-	900	0
3000	-	1,100	100
4000	-	1,400	1,000
5000	-	1,700	13,400
6000	-	2,100	18,200
	Titanium Target Plate		
	Test Data		
1500	500	600	1,000
2900	1300	1,500	600
4800	2300	5,200	14,300
	Smoothed Data		
1000	-	400	300
2000	-	800	800
3000	-	1,600	1,900
4000	-	3,000	4,400
5000	-	5,800	10,400
6000	-	11,200	24,200

- Data not obtained.

TABLE XVI. DEPLETED URANIUM (CONCLUDED)

Steel Target Plate

Test Data

Velocity (fps)		Thermal Energy (watt-sec/m^2)	
Initial	Residual	Front	Back
1400	500	700	200
3000	1300	1,400	7,000
4900	2200	4,800	11,400
	Smoothed Data		
1000	-	500	200
2000	-	900	700
3000	-	1,600	2,200
4000	-	2,700	6,900
5000	-	4,800	21,500
6000	-	8,400	67,000

- Data not obtained.

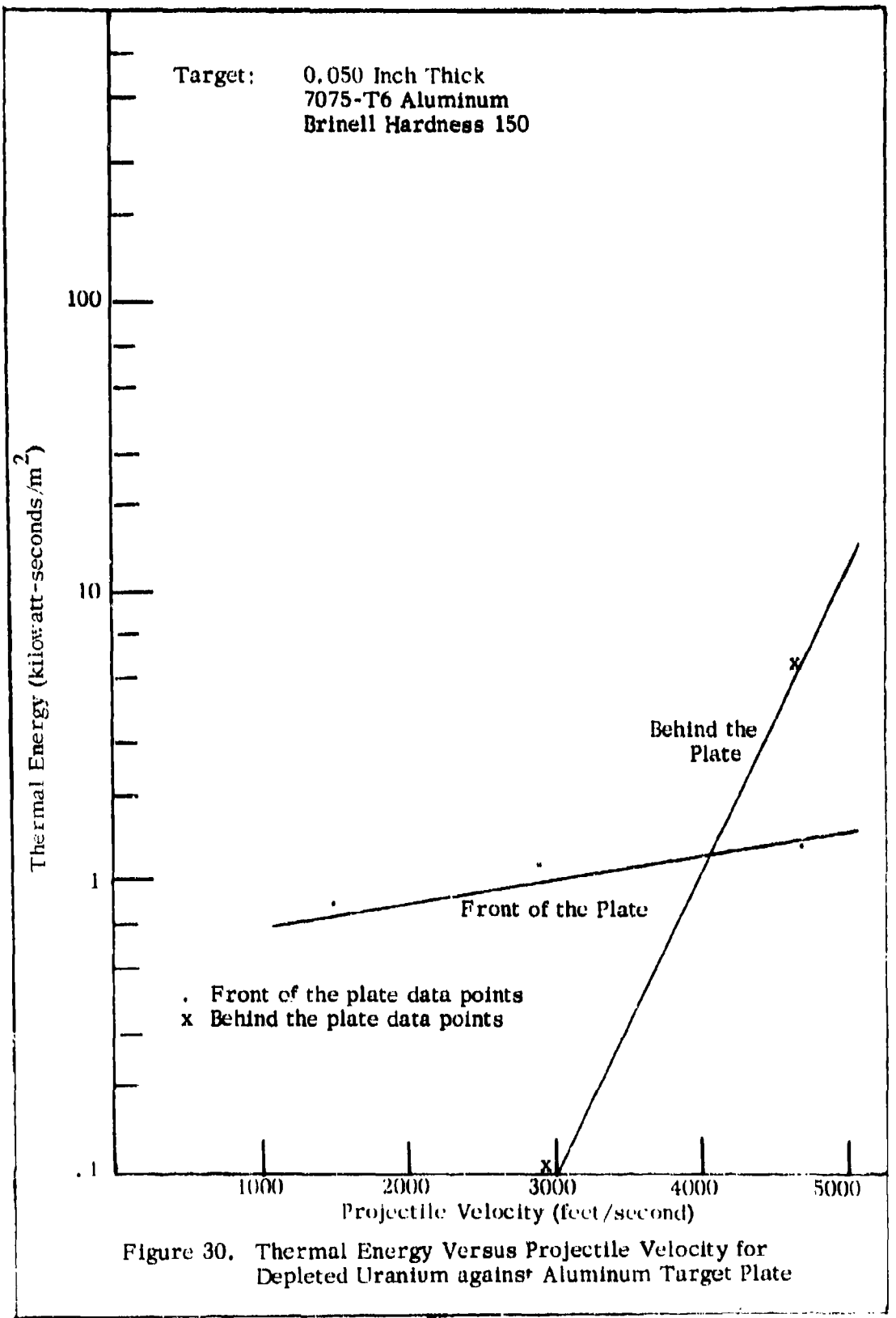

Figure 30. Thermal Energy Versus Projectile Velocity for Depleted Uranium against Aluminum Target Plate

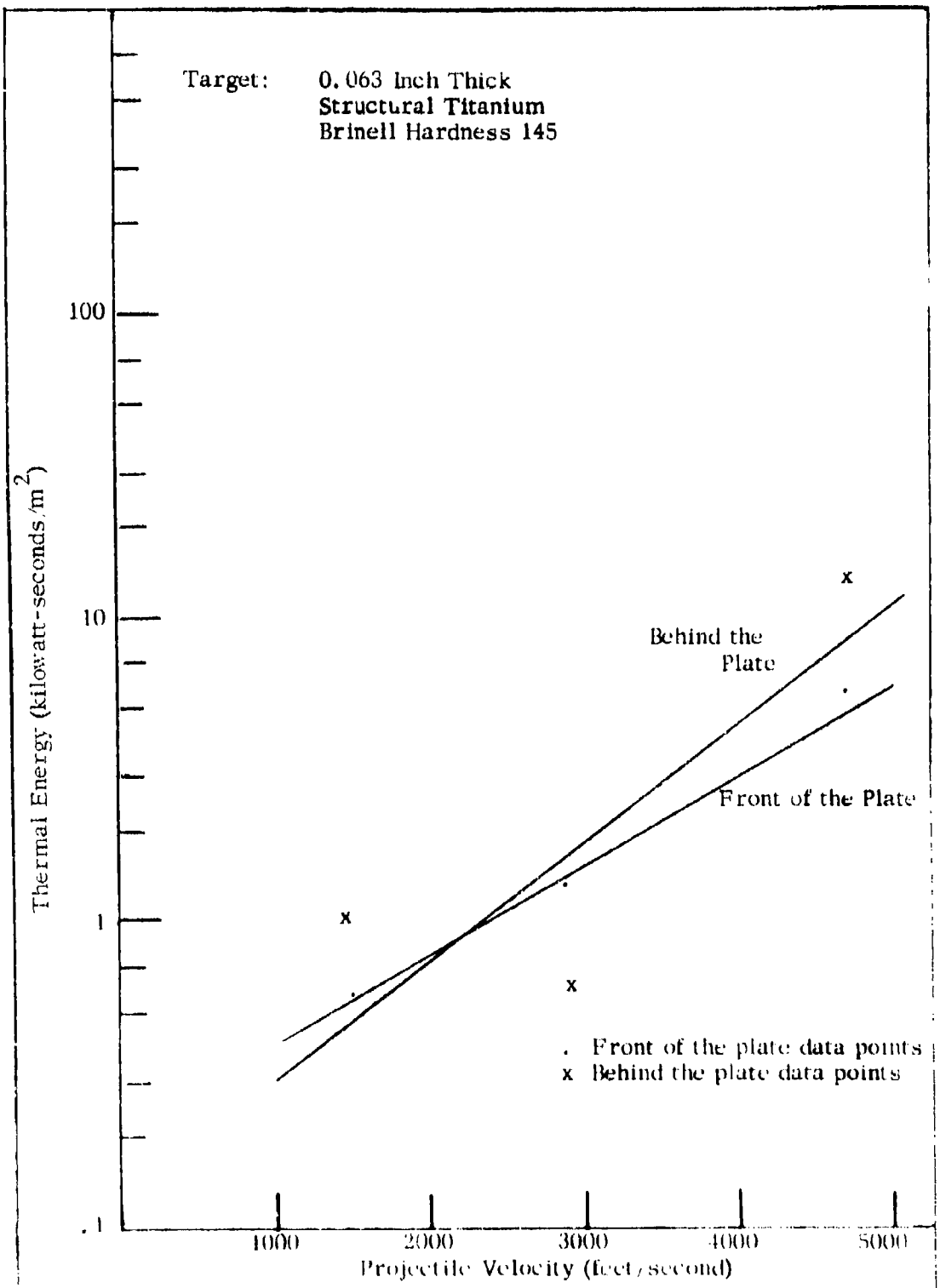

Figure 31. Thermal Energy Versus Projectile Velocity for Depleted Uranium against Titanium Target Plate

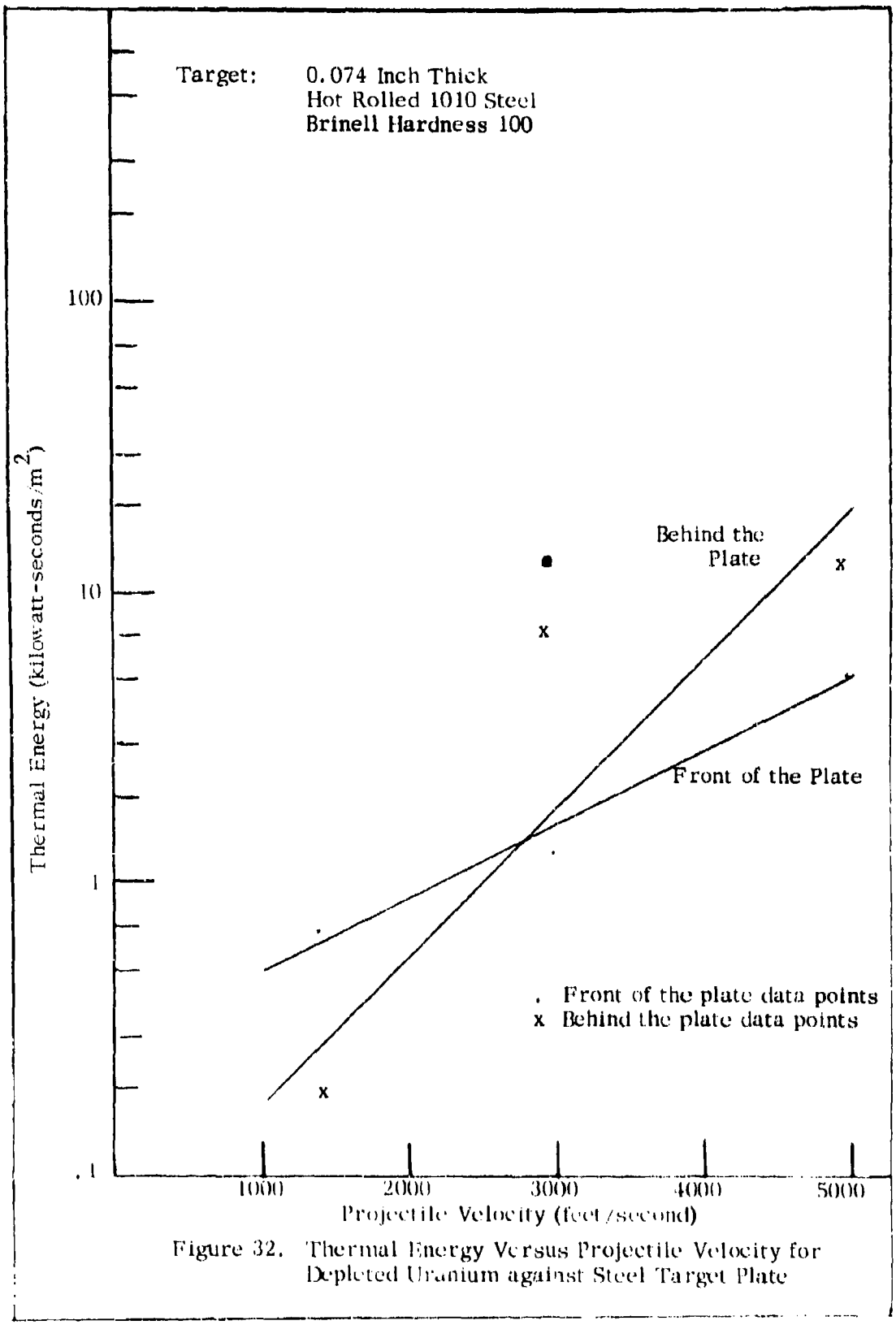

Figure 32. Thermal Energy Versus Projectile Velocity for Depleted Uranium against Steel Target Plate

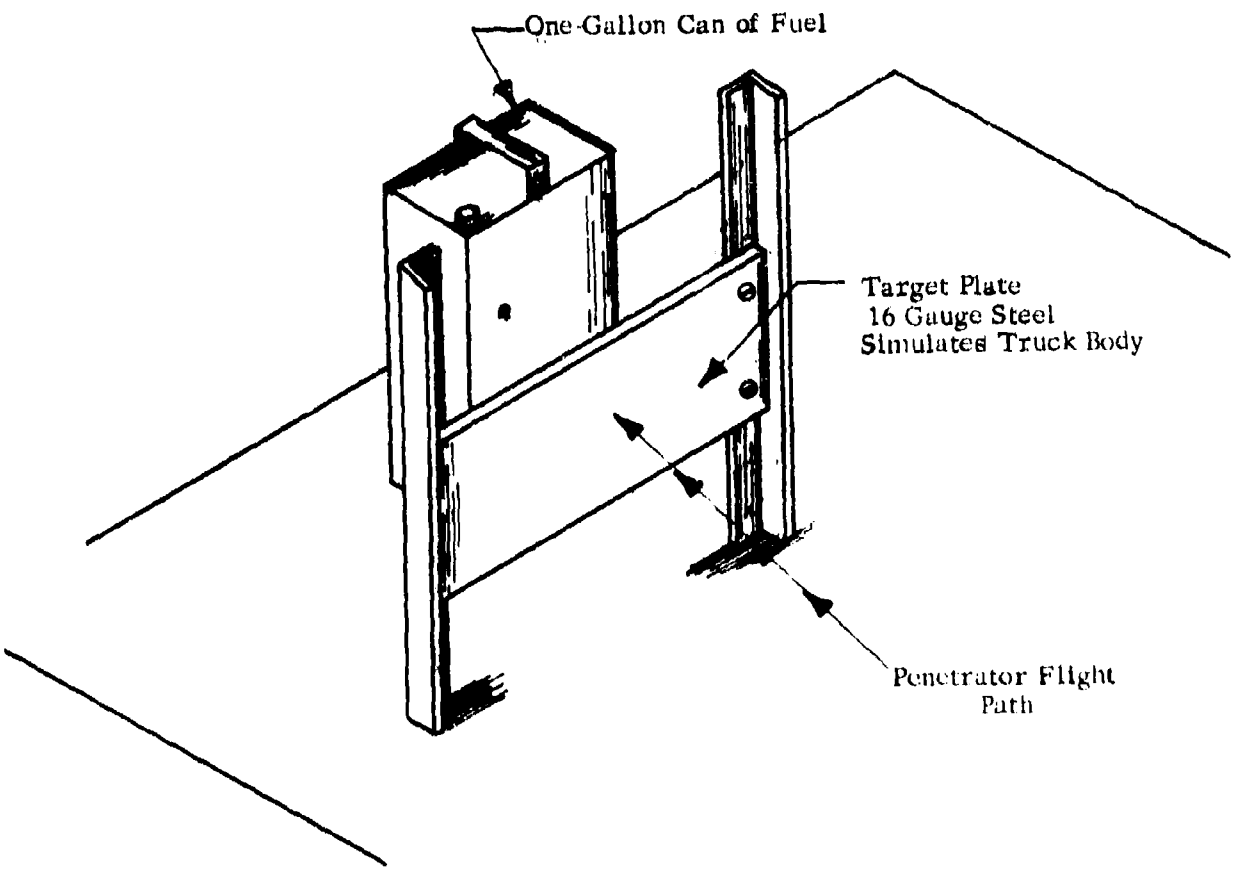

Figure 33. Simulated Truck Fuel Tank

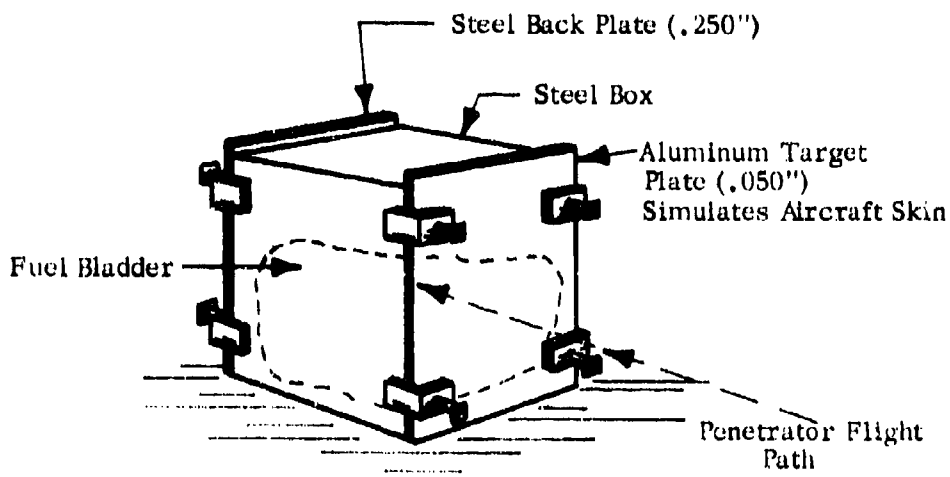

Figure 34. Simulated Aircraft Wing Tank

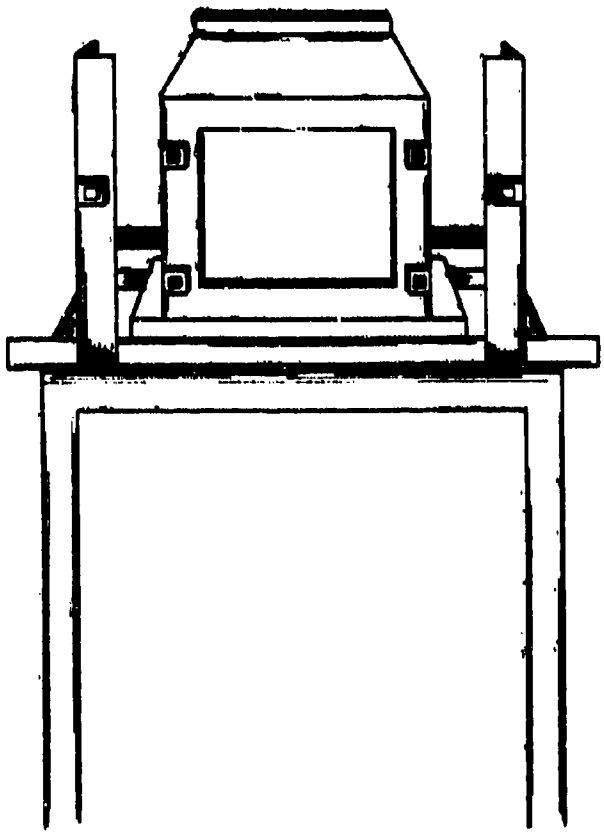

Figure 35. Simulated Wing Tank on Stand

TABLE XVII. RESULTS OF INCENDIARY TESTING (SIMULATED TRUCK TANK WITH MOGAS)

90% MRE + 10% Bismuth Penetrators

Velocity (fps)	Results	Velocity (fps)	Results
1800	Fire	2000	Fire
1800	Fire	2500	Fire

95% MRE + 5% Magnesium Penetrators

Velocity (fps)	Results	Velocity (fps)	Results
1600	No Penetration	2700	Fire
2100	Fire		

96% MRE + 4% Aluminum Penetrators

Velocity (fps)	Results	Velocity (fps)	Results
2000	Fire	2400	Fire

Zirconium Penetrators

Velocity (fps)	Results	Velocity (fps)	Results
1900	No Fire	2500	Fire
2500	No Fire	3000	Fire

Zirconium-Tin Penetrators

Velocity (fps)	Results	Velocity (fps)	Results
2000	No Fire	2600	Fire
2500	No Fire	3000	No Fire
2500	No Fire	3100	Fire
2600	Fire		

Depleted Uranium

Velocity (fps)	Results	Velocity (fps)	Results
2700	No Fire	4000	Fire
3300	No Fire	4000	Fire

TABLE XVIII. RESULTS OF INCENDIARY TESTING (SIMULATED WING TANK WITH KEROSENE)

90% MRE + 10% Bismuth Penetrators

Velocity (fps)	Results	Velocity (fps)	Results
3100	No Fire	3700	No Fire
3200	No Fire	3700	No Fire
3200	No Fire	3800	No Fire

95% MRE + 5% Magnesium Penetrators

Velocity (fps)	Results	Velocity (fps)	Results	Velocity (fps)	Results
2700	No Fire	3100	No Fire	3700	No Fire
2700	No Fire	3100	No Fire	3700	No Fire
2700	No Fire	3200	No Fire	3800	No Fire

96% MRE + 4% Aluminum Penetrators

Velocity (fps)	Results	Velocity (fps)	Results	Velocity (fps)	Results
2100	No Fire	2600	No Fire	3600	No Fire
2300	No Fire	2700	No Fire	3700	No Fire
2500	No Fire	3200	No Fire	3700	No Fire
2500	No Fire	3200	No Fire		

Zirconium Penetrators

Velocity (fps)	Results	Velocity (fps)	Results	Velocity (fps)	Results
3100	No Fire	3500	No Fire	5100	No Fire
3100	No Fire	3600	No Fire	5200	No Fire
3100	No Fire	3600	No Fire		

Zirconium - Tin Penetrators

Velocity (fps)	Results	Velocity (fps)	Results	Velocity (fps)	Results
3000	No Fire	3500	No Fire	5000	No Fire
3000	No Fire	3600	No Fire	5000	No Fire
3100	No Fire	3700	No Fire		

TABLE XIX. RESULTS OF INCENDIARY TESTING
(SIMULATED TRUCK TANK WITH KEROSENE)

90% MRE + 10% Bismuth Penetrators

Velocity (fps)	Results
2900	No Fire
3000	No Fire
3400	No Fire

TABLE XX. RESULTS OF INCENDIARY TESTING
(SIMULATED WING TANK WITH MOGAS)

Zirconium Penetrators

Velocity (fps)	Results	Velocity (fps)	Results
3500	Fire	3000	No Fire
3500	No Fire	3000	No Fire
3400	No Fire	3000	No Fire

Zirconium-Tin Penetrators

Velocity (fps)	Results	Velocity (fps)	Results
3590	No Fire	3100	No Fire
3470	No Fire	3060	No Fire
3410	No Fire	3030	No Fire

90% MRE + 10% Bismuth Penetrators

Velocity (fps)	Results	Velocity (fps)	Results	Velocity (fps)	Results
3700	No Fire	2500	Fire	1600	No Fire
3500	Fire	2300	Fire	1500	
		2300	Fire	1400	Fire
3000	Fire	2100	Fire	900	No Fire
2800	No Fire	2000	Fire	900	No Fire
2700	Fire	2000	Fire	800	No Fire

95% MRE + 5% Magnesium Penetrators

Velocity (fps)	Results	Velocity (fps)	Results	Velocity (fps)	Results
3100	No Fire	2600	No Fire	2100	No Fire
3000	Fire	2500	No Fire	2000	No Fire
3000	No Fire	2300	Fire	1800	No Fire

96% MRE + 4% Aluminum Penetrators

Velocity (fps)	Results	Velocity (fps)	Results
3100	Fire	2600	No Fire
3000	No Fire	2600	No Fire
2900	Fire	2500	No Fire

TABLE XXI. RESULTS OF FIRINGS AGAINST TWO IN-LINE STEEL TARGET PLATES

Zirconium Commercial

Velocity (fps)	First Target	Second Target	Recovery Pack
1500	Penetrated	Slight dent (impression)	-
1600	Penetrated	Slight dent	-
1800	Penetrated	Deep dent	-
3500	Penetrated	Penetrated	Fifth layer

Zirconium-Tin

Velocity (fps)	First Target	Second Target	Recovery Pack
1500	Penetrated	Slight dent	-
1600	Penetrated	Slight dent	-
1700	Penetrated	Good dent	-
2100	Penetrated	Penetrated	First Layer
3400	Penetrated	Penetrated	Fifth layer

96% MRE + 4% Aluminum

Velocity (fps)	First Target	Second Target	Recovery Pack
2300	Penetrated	Many small impressions	-
2500	Penetrated	Many small impressions	-
3600	Penetrated	Many small impressions fairly deep	-
3800	Penetrated	Many small impressions almost penetrated	-

90% MRE + 10% Bismuth

Velocity (fps)	First Target	Second Target	Recovery Pack
2600	Penetrated	Fused to second plate	-
3600	Penetrated	Many small frags fused to second target (almost penetrated)	-

95% MRE + 5% Magnesium

Velocity (fps)	First Target	Second Target	Recovery Pack
2900	Penetrated	Slight break	-
3600	Penetrated	Many small frags fused to plate (almost penetrated)	

- Did not penetrate recovery pack.

SECTION VI

CONCLUSIONS AND RECOMMENDATIONS

1. A comprehensive program of the research and production of 27 rare earth alloys was accomplished. Physical and thermochemical data were taken on alloys and are reported.

2. A comparison of the terminal effects of all pyrophoric metal penetrators, without bias to preferred or proprietary metals, was made against common structural materials: aluminum, titanium, and steel sheet.

3. A basis for the selection of a pyrophoric metal penetrator material as a function of projectile velocity and target material has been established.

4. The penetrator lower velocity limit for the sustained ignition of volatile fuels was determined for five selected materials against simulated fuel tank bladders.

On the basis of the above considerations, it is recommended that additional effort be directed to the following:

1. Thermal effects data on the gun-launched firings of penetrators of larger caliber.

2. Studies on the scaling effect of large caliber pyrophoric penetrators on the sustained ignition of low volatile motor and jet fuels.

3. Design effects of the penetrator configuration (blunt nose, cookie cutter, etc.) on the ballistic limit and subsequent break up and heat pulse duration.

REFERENCES

1. G. H. Custard, G. Francis, and W. Schnackenberg, Small Arms Incendiary Ammunition, A Review of the History and Development, AD 159323, December 1956.

2. F. H. Spedding and A. H. Daane (Editors), The Rare Earths, John Wiley and Sons, New York (1961).

3. Karl A. Gschneidner, Jr., Rare Earth Alloys, D. Van Nostrand Company, Princeton, New Jersey (1961).

APPENDIX A

DYNAMIC TEMPERATURE AND HEAT MEASUREMENT

Pyrometers have the capability to measure rapidly changing temperatures as observed when a pyrophoric material impacts with high impulse.

Detectors with time constants as low as 10 μsec are available for use in measuring rapidly varying temperatures as low as 100°C. Time distributions of temperature can be obtained through the use of an oscillograph fitted with a camera. The photographs give a permanent calibrated record of the time-temperature profile.

Radiation pyrometers and optical pyrometers are the most widely used classes of pyrometers for measuring transient temperatures.

Optical pyrometers usually employ a sensitive semiconductor or photomultiplier as the detector. The detector is normally filtered with a narrow bandpass to be centered at 650 mμ or 467 mμ. Radiation pyrometers also function in the same manner but usually employ detectors more sensitive to longer infrared wavelengths and use wider bandpasses about the filter centerpoint. Temperatures obtained with these types of optical and radiation pyrometers are referred to as "Brightness" temperature and represent the temperature at which a blackbody must be to emit the same amount of radiation as the target being measured.

Once the "Brightness" temperature of a target is determined it is known from the Planck formula that such a temperature is the lowest possible temperature of the target, integrated over the field of view of the pyrometer. If the emissivity, or a reasonable estimate of the emissivity is known, the "Brightness" temperature can be adjusted to approach the "true" temperature value by the following variation of the Planck formula.

$$T_{tr} \simeq \frac{T_{br}}{T_{br}\left(\frac{k\ \lambda}{hc_o}\right) \ln\epsilon + 1}$$

where k = Boltzmann's constant = 1.3805×10^{-23} joules/deg K and h = Planck constant = 6.6252×10^{-34} joule sec.

ϵ = Emissivity ≤ 1

λ = Wavelength

c_o = Speed of Light = 2.9979×10^{8} m/sec

T_{br} = Brightness Temperature

T_{tr} = True Temperature

It can be observed from this formula that as the emissivity (ξ) approaches unity T_{tr} approaches T_{br} and that at $\xi = 1$ the value for T_{tr} is at a minimum.

It becomes apparent that the "True Temperature" of a target cannot be determined pyrometrically unless an accurate value for its emissivity is known.

In the case of impact flashes from pyrophoric materials it would be far beyond the scope of this program to attempt to define the emittance values for the combustion products of the pyrophoric materials being studied.

It is meaningful, however, to use these "Brightness" temperature to represent the minimum temperature as integrated over the field of view of the pyrometer.

Additionally, radiation pyrometers such as those used in this study may function as radiometers to measure radiated power as well as temperature since such pyrometers are actually radiation sensors. To be utilized as radiometer the pyrometer must of course be calibrated against a suitable radiation standard in much the same manner as it is calibrated against a temperature standard when used to measure temperatures.

The radiation standard utilized to calibrate the pyrometers in this study was an AFATL blackbody traceable to the Bureau of Standards.

Thereby the pyrometers were able to sense both temperature and radiated power of impact events as a function of time. These events were recorded on films of oscilloscope traces as previously described in the body of the report (Figure 14). The traces therefore are histories of the temperature and radiated power, both as a function of time as observed by the field of view of the pyrometers.

The peak of the trace represents the maximum temperature of the event and the "Brightness Temperature".

The area under the curve traced is a measurement of the time integral of radiated power (watt-sec per meter^2)* and thereby a measurement of the mechanical equivalent of heat of the event.

* The field of view of the pyrometers used in this study at the plane of the penetrator trajectory was 0.0165 square meter.

(The reverse of is page is blank)

INITIAL DISTRIBUTION

DIR, DASA (TECH LIB)	1	DLM	1
HQS USAF (AFTAC/TD-5)	1	DLRD	1
HQS USAF (SAFAAE)	1	DLD	1
AFSC (SDSM)	2	DLRV	5
ASD (TWT)	1		
ASD (ENYS)	1		
ASD (XRH)	1		
ASD (ENVW)	1		
AFIT (ENB)	1		
AFCRL (CRSAM)	1		
CH R&D (ORCD)	1		
PICATINNY ARS, AMSMU-SS-SC	1		
PICATINNY ARS, SMUPA-DW8	2		
FRANKFORD ARS (LIB)	1		
USA WPNS CMD AMSWE-RDW	1		
USA R&D CTR (AMXRD-AW)	1		
BRL (AMXRD-BTL)	2		
BRL (AMXBR-XBL)	1		
BRL (AMXRD-BVL)	1		
NAV ORD SYS CODE ORD-0332	1		
USN ORD STA	2		
USNWC CODE 501	2		
USNWC CODE 505	1		
USNWC CODE 4561	1		
USNWC CODE 40708	1		
USN WPNS EVAL FAC (CODE WE)	1		
DIR USAF PROJ RAND	2		
DDC	2		
BATELLE MEM INST	1		
AEROSPACE CORP	1		
SACPO	1		
TAWC-DT	1		
AUL (AUL-LSE-70-259)	1		
HQ PACAF (IGY)	1		
TRADOC/ADTC/DO	1		
DL	1		
DLB	1		
DLKS	1		
DLG	1		
DLDG	1		
DLX	1		
DLWT	1		
DLY	1		
DLW	1		
DLI	1		
DLR	1		
DLIF	3		
DLOSL	2		
	1		

(The reverse of this page is blank.)

UNCLASSIFIED

Security Classification

DOCUMENT CONTROL DATA - R & D

(Security classification of title, body of abstract and indexing annotation must be entered when the overall report is classified)

1 ORIGINATING ACTIVITY (Corporate author)

Ordnance Research, Inc.
Fort Walton Beach, Florida 32548

2a. REPORT SECURITY CLASSIFICATION
UNCLASSIFIED

2b. GROUP

3 REPORT TITLE

STUDY OF THE TERMINAL EFFECTS OF PYROPHORIC METAL FRAGMENTS

4 DESCRIPTIVE NOTES (Type of report and inclusive dates)
Final Report - September 1970 to February 1973

5 AUTHOR(S) (First name, middle initial, last name)

Hal R. Waite
Theodore B. Gortemoller

6 REPORT DATE	7a. TOTAL NO. OF PAGES	7b. NO. OF REFS
February 1973	97	3

8a. CONTRACT OR GRANT NO.	9a. ORIGINATOR'S REPORT NUMBER(S)
F08635-71-C-0020	
b. PROJECT NO. 670A	
c. Task No. 07	9b. OTHER REPORT NO(S) (Any other numbers that may be assigned this report)
d. Work Unit No. 01	AFATL-TR-73-26

10 DISTRIBUTION STATEMENT

Distribution limited to U. S. Government agencies only; this report documents test and evaluation; distribution limitation applied February 1973 . Other requests for this document must be referred to the Air Force Armament Laboratory (DLRV), Eglin Air Force Base, Florida 32542.

11 SUPPLEMENTARY NOTES	12 SPONSORING MILITARY ACTIVITY
Available in DDC	Air Force Armament Laboratory Air Force Systems Command Eglin Air Force Base, Florida 32542

13 ABSTRACT

Thirty-three metals and alloys having pyrophoric properties were surveyed for applicability as gun-launched kinetic energy penetrators, incendiaries, and fuel igniters. Using actual samples physical properties were determined, ignition combustion termperature/burn time profiles were established, and dynamic terminal effects were tested. Three final candidates were tested against simulated characteristic targets. The results of all testing are tabulated, and recommendations are made for an advanced development program.

DD FORM 1 NOV 65 1473

UNCLASSIFIED

Security Classification

KEY WORDS	LINK A		LINK B		LINK C	
	ROLE	WT	ROLE	WT	ROLE	WT
Pyrophoric Metal Fragments						
Terminal Effects						
Gun-Launched Kinetic Energy						
Incendiaries						
Fuel Igniters						
Ignition-Combustion Temperature/Burn Time Profiles						
Dynamic Terminal Effects						